NASA
Technical
Paper
1995

May 1982

Aeroacoustic Performance of an Externally Blown Flap Configuration With Several Flap Noise Suppression Devices

Daniel J. McKinzie, Jr.

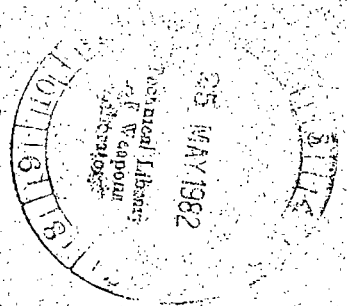

NASA

NASA Technical Paper 1995

1982

Aeroacoustic Performance of an Externally Blown Flap Configuration With Several Flap Noise Suppression Devices

Daniel J. McKinzie, Jr.
Lewis Research Center
Cleveland, Ohio

NASA
National Aeronautics and Space Administration

Scientific and Technical Information Branch

Summary

Small-scale model acoustic experiments were conducted to measure the noise produced in the flyover and sideline planes by an engine under-the-wing externally blown flap configuration in its approach attitude. Broadband low-frequency noise reductions as large as 9 dB were produced by reducing the separation distance between the nozzle exhaust plane and the flaps. Experiments were also conducted to determine the noise suppression effectiveness in comparison with a reference configuration of three passive types of devices that were located on the jet impingement surfaces of the reference configuration. These devices produced noise reductions that varied up to 10 dB at reduced separation distances. In addition, a qualitative estimate of the noise suppression characteristics of the separate devices was made. Finally static aerodynamic performance data were obtained to evaluate the penalties incurred by these suppression devices. The test results suggest that further parametric studies are required in order to understand more fully the noise mechanisms that are affected by the suppression devices used in this study.

Introduction

Three major problems affecting the future viability and growth of the air transportation industry are aircraft noise, aircraft engine exhaust pollution, and aircraft congestion (ref. 1). A new air transportation system considered promising for the relief of air traffic density is the short-haul powered-lift aircraft system which would operate from relatively short runways. This system uses the wing and flaps to deflect the engine exhaust downward to achieve powered lift. Two powered-lift concepts have been considered; one required mounting an engine under-the-wing (UTW), while the other was designed for an over-the-wing (OTW) installation. The UTW engine in the powered-lift mode is an example of an externally blown flap (EBF) system, while the OTW engine in powered-lift operation is an example of an upper-surface-blown (USB) system. This report is concerned only with the engine UTW installation shown schematically in figure 1. Because of the impingement of the jet exhaust flow on the wing and flap surfaces of this concept, sound levels from 10 to 18 dB greater than the undeflected jet exhaust alone can be generated (refs. 2 and 3).

NASA has conducted research and development studies to measure and define the jet-flap interaction sound field for a variety of engine UTW EBF configurations (ref. 4). These studies showed that the interaction noise varied nominally with the sixth power of jet velocity. Thus, engine design studies were conducted (ref. 1) that proposed the use of low pressure ratio high bypass ratio turbofan engines in order to produce significant reductions in jet velocity and, consequently, low interaction noise. Yet in such powered-lift concepts as the Quiet Clean Short-haul Experimental Engine (QCSEE) propulsion system (ref. 5) even with these low jet velocities, jet-flap interaction noise is still a major problem. As a result, a need for noise suppression techniques was established in order to meet the proposed noise goal of 95 effective perceived noise decibels (EPNdB) at a 152.4-meter sideline distance for powered lift aircraft (ref. 2).

Any proposed jet-flap interaction noise suppression concept must be compatible with other operational design requirements. Among these requirements are good jet-flap lift augmentation characteristics, low structural vibration, low cruise interference drag, low weight, and structural simplicity. In addition, the noise producing mechanisms and scaling laws must be known for each of the active noise sources, at least approximately, in order to ensure that the most dominant will, in fact, be suppressed successfully. Once these mechanisms are known, the challenge of determining how to suppress the noise sources remains. At the present time, there are phenomenological studies reported in the literature, which have supplied some understanding of the noise source mechanisms involved in the UTW EBF configuration, but there has been very little methodology published demonstrating how suppression of these noise sources may be successfully accomplished. This lack of methodology has been caused, in part, by adverse changes in the flow field and the concurrent acoustic field when suppression devices have been added to the wing-flap system. Available information includes the work reported in reference 6 using a small scale three-flap UTW EBF model, and that in references 7 and 8 using a large-scale two-flap model. In these studies passive types of suppression devices were used. The results show overall sound pressure level reductions amount to between 3 and 5 dB. Corresponding spectral data show

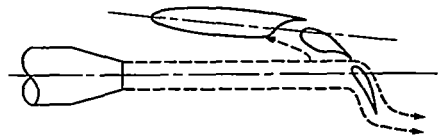

Figure 1. - Schematic of externally blown flap in approach attitude with conical nozzle.

that these reductions occurred in a restricted frequency range about the peak of the spectra resulting in only small reductions in perceived noise level. Although these tests demonstrated that passive suppression devices could be used to suppress noise, they also showed that the knowledge needed to arbitrarily suppress a particular spectral and/or spacial characteristic of jet-flap interaction noise was not available.

An analysis of the two flap EBF noise sources is presented in reference 8. The analysis indicates that in the approach attitude the dominant noise directly beneath the nozzle, wing, and flaps is impact noise, produced by the impingement of the jet exhaust on a sufficiently large flap surface (ref. 9). Two remaining important noise sources are fluctuating lift noise (in-flow noise), produced by a fluctuating lift response of an airfoil to an upwash disturbance; and trailing-edge noise, produced by the flow passing over the trailing edge of the most downstream flap. This analysis also indicates that, for an externally blown flap in the approach attitude, the scaling laws for the three dominant noise sources are not the same. Thus, one must be cautious in applying any universal scaling law to small scale test results. It is suggested in reference 8 that the frequency at which the peak sound pressure level occurs may be governed by the periodic formation and shedding of the large-scale turbulence structures, discussed in reference 10, that originate at the exit plane of the exhaust nozzle. It is further suggested that these turbulence structures are simultaneously responsible for producing impact and fluctuating lift noise. The large-scale turbulence structures are represented as toroidal vortex rings, which are convected downstream by the jet flow field. These rings expand and grow in size as the jet mixing layer grows. The large-scale turbulence structures extract energy from the mean jet flow and this gain is balanced by viscous dissipation in the self-preserving flow field, which starts at a point downstream from the nozzle exit greater than 5 nozzle diameters. Thus, between the nozzle exit and at least 5 nozzle diameters downstream, the turbulent energy spectrum would be expected to be dominated by the energy contribution of the large-scale turbulent structures.

In references 8 and 9, it is proposed that by positioning the flaps closer to the nozzle exit plane, possibly to within 2 nozzle diameters, the flaps would intercept smaller large-scale turbulence structures. The following enumerated advantages may result from this procedure: first, interaction of the flaps with the lower turbulence intensity of the jet core flow at this location; second, improved noise suppression by devices applied to the flaps because these devices intercept more of the flow field before spreading and mixing effects occur; and third, a significant reduction in the size of the large-scale turbulence structures (modeled in ref. 10 as bounded by the size of the flow field) impacting the flaps would result in an attenuation of the broadband low-frequency jet-flap interaction noise. In addition, a more recent theoretical analysis of an engine UTW EBF system in reference 11 indicates that the noise output in the low-frequency region of the spectrum is strongly dependent on the nozzle-to-flap axial separation distance. This result indicates that, by reducing the separation distance, the sound levels in the low-frequency region of the spectrum can be reduced.

Therefore, because of the successful use of the passive noise suppression devices referred to in references 6 to 8 and the indication in references 8, 9, and 11 that additional suppression benefits may be obtained at reduced nozzle-to-flap separation distances, the first of four objectives of this study is to compare the spacial distribution and spectra of the noise produced by a small-scale model two-flap UTW EBF in the approach attitude at reduced nozzle-to-flap separation distances with a reference configuration. The approach attitude was chosen because it produces more flap noise than the takeoff attitude for the same jet velocity, thus making it easier to observe the suppression effects. The second objective is to demonstrate both spectrally and spacially the noise suppression effectiveness of several passive types of suppression devices applied singularly and in combination to the EBF approach configuration at reduced nozzle-to-flap separation distance. This is done by comparing the noise produced by the configurations equipped with the noise suppression devices to the noise produced by the reference configuration shown in figure 2. The reference configuration does not represent an "optimum" design. It is, however, representative of typical proposed designs, discussed in reference 3, that require suppression in order to meet proposed noise goals. It should be noted that just because a feature of the total noise is suppressed by a particular device, the effect of the device on the noise sources cannot be quantitatively assessed without a decomposition of the sound spectrum, which is beyond the scope of this report. Consequently, no attempt will be made to quantify the noise suppression characteristics of the separate devices used in these tests. However, the third objective is to

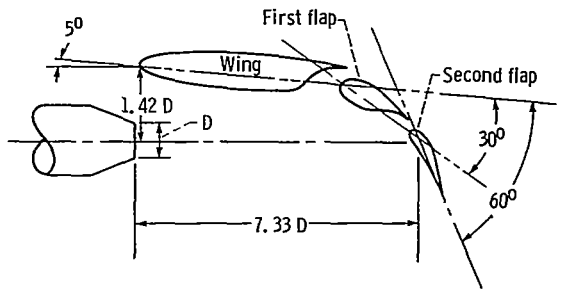

Figure 2. - Reference configuration in approach attitude (D = 5.08 cm).

estimate qualitatively the noise suppression characteristics of the devices used alone and in combination as a function of the nozzle to flap separation distance. Finally, the fourth objective is to compare the static aerodynamic performance data including the jet exhaust turning efficiency of each configuration with that of the reference configuration. Also, a qualitative estimate of the change in static aerodynamic performance parameters produced by each of the suppression devices is made.

Test Facilities and Models

Test Facilities

Anechoic chamber flow system.—The acoustic test stand, used to obtain the acoustic data presented in this report, was located in the Lewis Research Center's Engine Fan and Jet Noise Facility shown schematically in figure 3. The mass flow metering system supplying cold air to the stand included a flow control valve and flow metering run. The total temperature varied throughout the test between 294 and 300 K and the anechoic chamber ambient temperature varied between 290 and 303 K. The valve noise quieting elements in the flow system consisted of a perforated plate followed by a tubular, no-line-of-sight muffler. As discussed in reference 12, jet noise test data obtained with this rig are not affected by internal valve noise down to jet velocities of 120 meters per second.

Acoustic instrumentation.—Eleven condenser microphones (0.64 cm in diameter) were placed along a 3.05-meter-radius semicircle in the horizontal plane and centered on the nozzle exit (fig. 3). The microphones and nozzle centerline were 3.05 meters above the tops of the fiberglass acoustic wedges on the floor of the facility. The microphones were located at angles of 20°, 40°, 50°, 60°, 70°, 80°, 90°, 100°, 110°, 115°, and 120° from the nozzle upstream axis, as shown in figure 3. With the exceptions of the microphones located at 115° and 120°, in the flyover plane, the microphones were used without grids. Grids and windscreens were necessary for the 115° and 120° microphones because the outer edge of the jet shear layer, deflected by the EBF model, impinged on these microphones.

The microphones were calibrated before each day of testing, and the one-third octave band analyzer was calibrated each day from 50 hertz and 100 kilohertz with a white noise source. Measurements were made in two planes relative to the model by repositioning the model, as described in the data section of this report.

Lift and thrust facility.—Static thrust and lift measurements were taken in a separate facility described in reference 13. The test stand was supplied with pressurized air at about 283 K. The air was supplied to a cylindrical plenum by two horizontally opposed supply lines. Flexible couplings in each supply line isolated the supply from a force measuring system. The plenum and any hardware attached to it were free to move axially and laterally by means of an overhead cable suspension

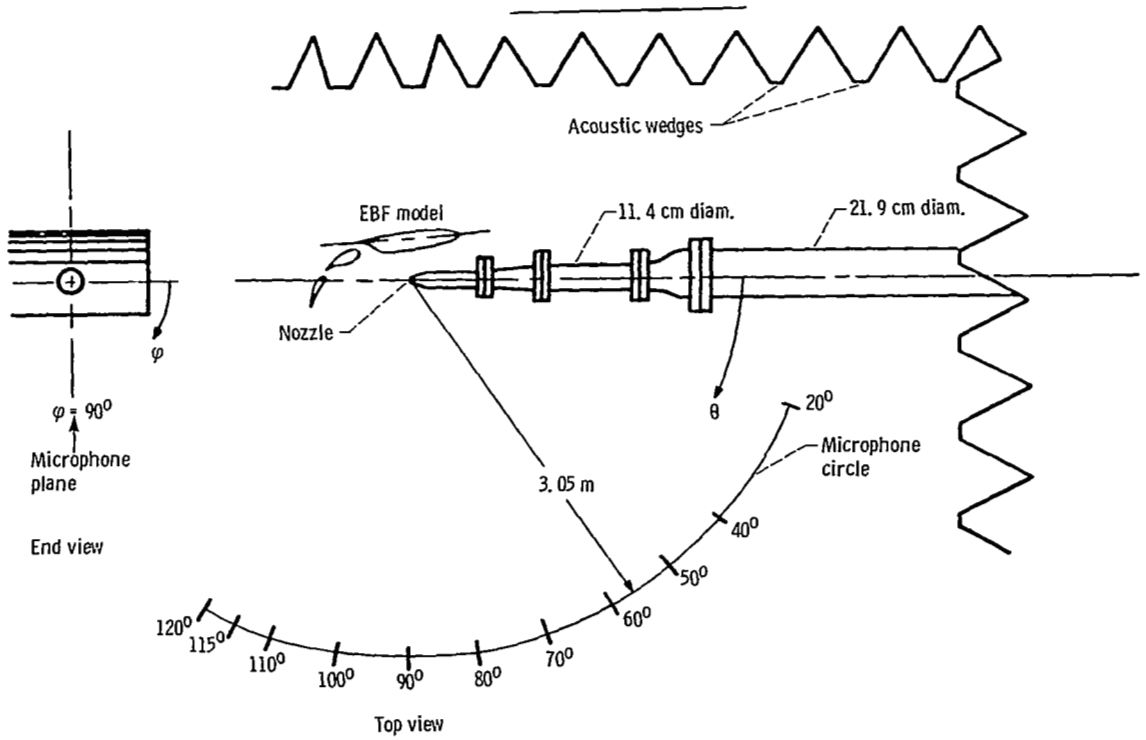

Figure 3. - Test rig in Engine Fan and Jet Noise Facility showing test model in approach attitude. Flyover plane, $\varphi = 90^{\circ}$.

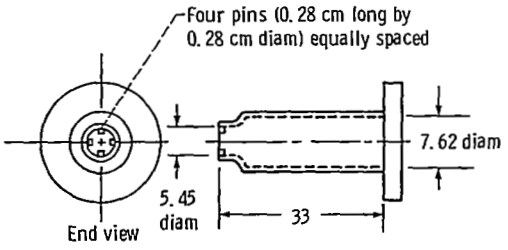

(a) Nozzle with pins in throat (used for X/D of 2 and 4).

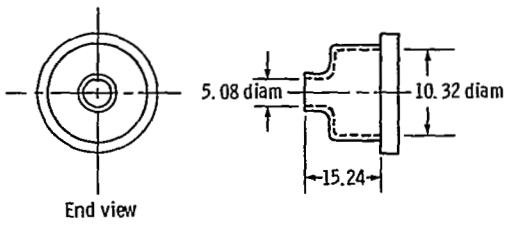

(b) Nozzle without pins in throat (used for X/D of 7.33).

Figure 4. - Convergent nozzle. (All dimensions in cm.)

system. The UTW EBF model and nozzles were attached to the plenum at the downstream end with the span of the wing in the vertical plane. The axial thrust was measured by a load cell at the upstream end of the plenum. Horizontal sideloads (forces normal to the jet axis) were measured by a second load cell mounted closer to the nozzle.

Model Description

Nozzles.—Two convergent circular nozzles (fig. 4) were used in the experiments in order to cover the range of nozzle-to-flap separation distances desired. Both nozzles were designed to provide the same nominal mass flow for like gas dynamic conditions. One nozzle had a throat diameter of 5.45 centimeters, while the other nozzle had a throat diameter of 5.08 centimeters. Four equally spaced pins 0.28 centimeter long by 0.28 centimeter in diameter were positioned at the exit plane of the 5.45-centimeter-diameter nozzle resulting in an effective diameter of 5.41 centimeters. This nozzle was specifically designed to inhibit the feedback mechanism of jets (ref. 10) that occurs at small nozzle-to-flap separation distances. Based on mass flow calibration

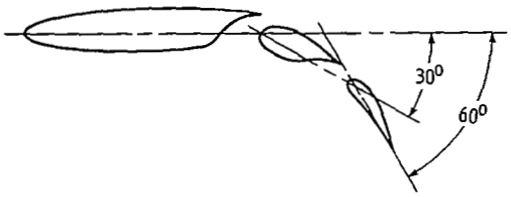

Configuration 1 unsuppressed

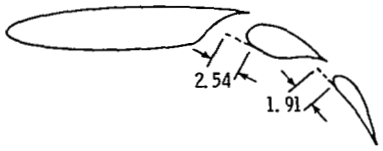

Configuration 4 with screens across slots

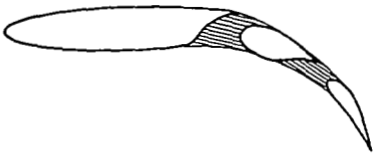

Configuration 2 with plugs in slots

Configuration 5 with ramp trailing edge screen

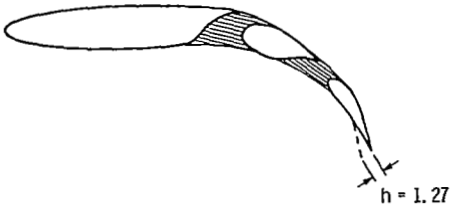

Configuration 3 with plugs in slots and ramp trailing edge screen

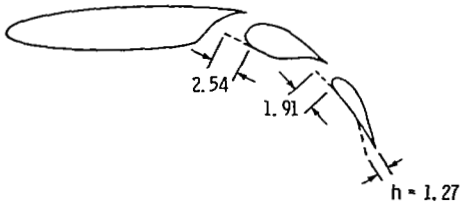

Configuration 6 with screen across slots and ramp trailing edge screen

Figure 5. - Experimental configurations in approach attitude. (All dimensions in cm unless indicated otherwise.)

measurement, the effective throat diameters of the nozzles with and without pins were 5.13 centimeters and 4.97 centimeters, respectively. The acoustic data were corrected to the smaller effective nozzle throat diameter of 4.97 centimeters using the scaling laws discussed in reference 14.

EBF configurations.—Six configurations using the noise suppression devices singularly and in combinations were investigated. The noise suppression effectiveness of these configurations was determined by comparison with the reference configuration. A schematic representation of the reference configuration is presented in figure 2. The nozzle-to-flap separation distance, measured along an extension of the nozzle axis, is 7.33 nozzle diameters.

The six configurations investigated in this study are shown schematically in figure 5. The approach attitude was used for all the tests. The six configurations and the reference configuration are treated separately. Configuration 1 consists of the same wing and flap model as the reference configuration, but was operated at reduced separation distance between the nozzle exit plane and the flaps. This specific configuration is referred to herein as the unsuppressed configuration because no mechanical suppression devices are used. Three types of passive suppression devices, located on or in between the flaps of the EBF, are used in configurations 2 to 6, which are referred to herein as the suppressed configurations. The devices were applied singularly or in combination, as shown in figure 5.

Configuration 2 is schematically shown in more detail in figure 6. Two short spanwise fairings were positioned between the wing and flaps. These fairings are referred to hereinafter as plugs or as plug fairings. Fairings similar to these were used in the large-scale acoustic tests reported in reference 8. They were centered in the spanwise plane in relation to the intersection of the nozzle axis with the flaps, and were designed to prevent most of the impinging jet flow from passing through the slots between the wing and the flaps.

Details of configuration 3 are shown in figure 7. This configuration had a screen fashioned as a ramp positioned on the trailing edge of the most downstream

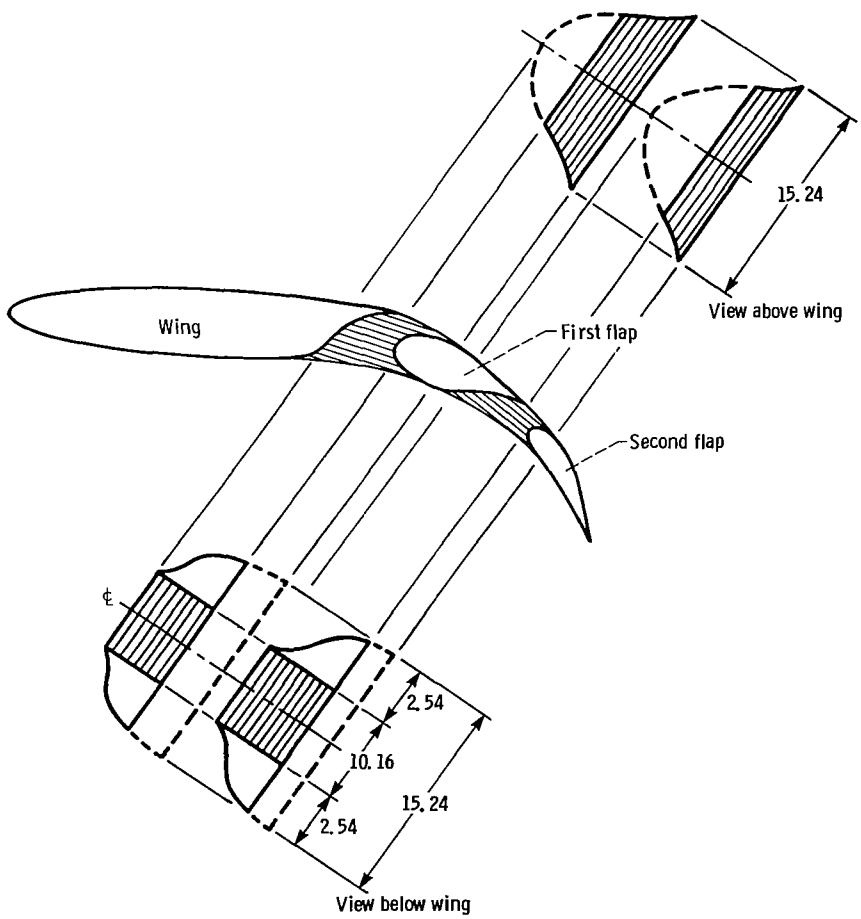

Figure 6. - Details of plug fairings in slots between wing and flaps of configuration 2. (All dimensions in cm.)

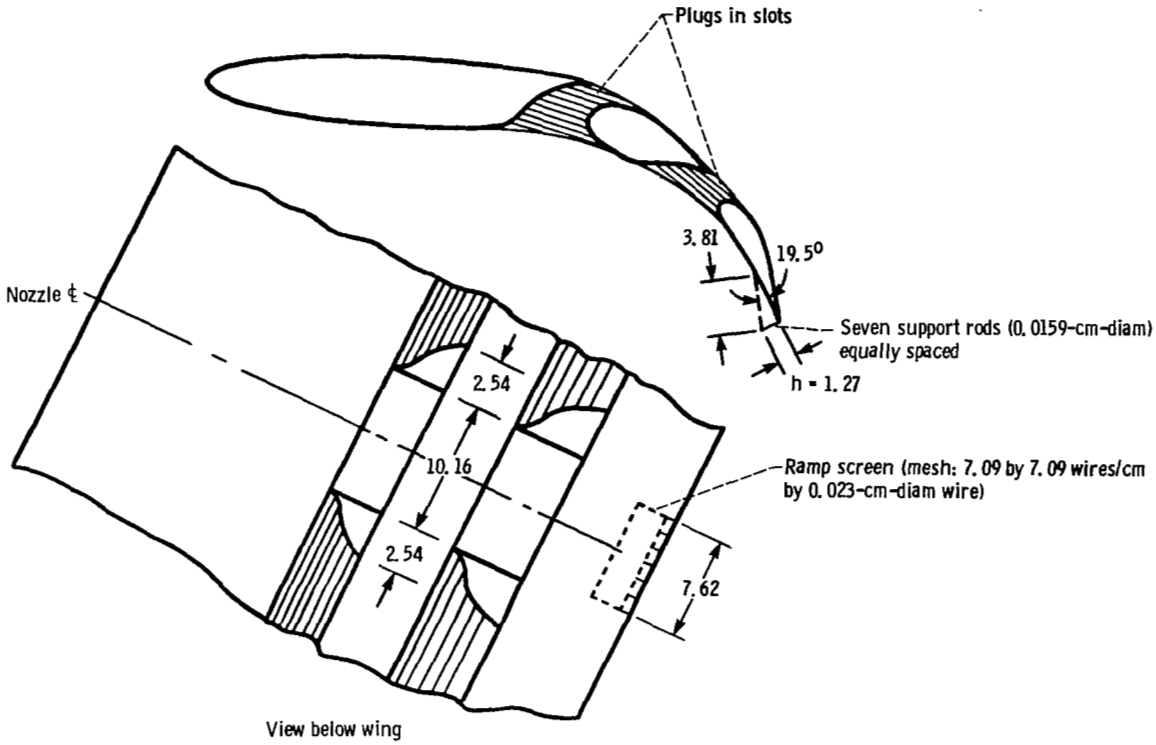

Figure 7. - Ramp screen installation used in configuration on trailing edge of second (most downstream) flap. (All dimensions in cm unless indicated otherwise.)

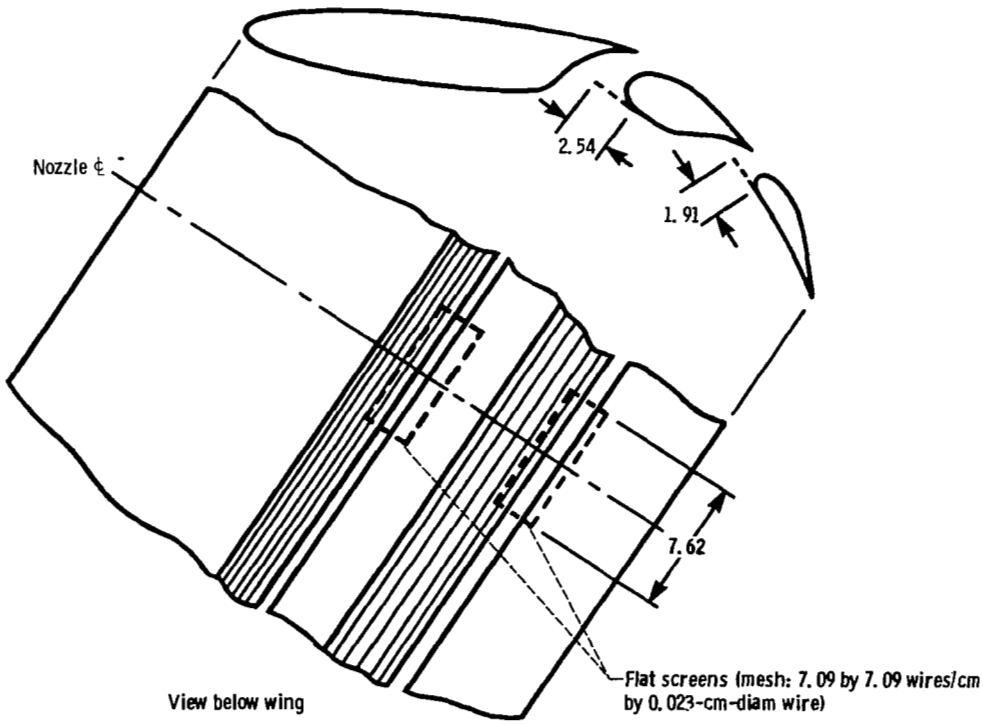

Figure 8. - Flat screen installation across slots between wing and flaps of configuration 4. (All dimensions in cm.)

flap, in addition to the plug fairings located in the slots between the wing and flaps. The screen was ramped up from the flap surface at an angle of 19.5° to a height of 1.27 centimeters. The trailing edge of the screen was supported by seven equally spaced rods of 0.16 centimeter diameter. The screen had a mesh of 7.09 by 7.09 wires per centimeter with a wire diameter of 0.023 centimeter.

Configuration 4 was designed specifically to permit a restricted flow through the flap openings. Screens were substituted in place of the plug fairings used in configurations 2 and 3 so that a small controlled amount of flow would pass over the upper surfaces of the flaps. Therefore, configuration 4 had a flat screen positioned over each of the slots between the wing and flaps as shown in figure 8. These screens were positioned in relation to the nozzle axis in the same way as the plug fairings. The screens were supported by seven rods (not shown) positioned in the chordwise plane and equally spaced along the spanwise dimension of the screens. Each of the rods had a diameter of 0.16 centimeter.

Configuration 5 had only a ramped screen located on the trailing edge of the second flap. Finally, configuration 6 had a ramped screen located on the trailing edge of the second flap, in addition to the flat screens positioned over the slots between the wing and flaps. Each of these screens had a wire mesh of 7.09 by 7.09 wires per centimeter, a wire diameter of 0.023 centimeter, and spanwise length of 7.62 centimeters.

Nozzle-to-flap positioning.—In order to determine the effect of jet-flap separation distance on the impingement noise, experiments were conducted generally at nozzle-to-flap separation distances X/D of 7.33, 4, and 2. The separation distance X was measured along the nozzle axis to a point where it intersected the second flap. The nozzle diameter D was 5.08 centimeters. The separation distances of 2 and 4 are referred to herein as reduced separation distances. The reference configuration, to which all the suppressed configurations are compared, had a separation distance of 7.33 nozzle diameters.

Data

Acoustic data were obtained along a 3.05-meter-radius semicircle in both the flyover and sideline planes. The flyover plane is perpendicular to the span of the wing, as shown in figure 3. The sideline plane is inclined 22° below a plane passing through the span of the wing and parallel to the axis of the nozzle.

The measured sound was processed by an automated spectrum analyzer which produced one-third octave band sound pressure levels referenced to 2×10^{-5} N/m^2 between 200 and 80 000 hertz. These data were corrected for effects of atmospheric attenuation (ref. 15), thus making them lossless. The lossless data were summed between 200 hertz and 40 kilohertz to obtain overall sound pressure levels which are considered free field and reliable (ref. 16). The spectral data above 40 kilohertz are presented here for information.

Overall sound pressure levels for each configuration are presented as a function of radiation angle θ (see fig. 3) between 20° and 120° referenced to the upstream jet axis. During aircraft approach (2° angle of attack of the wing chord, as noted in ref. 8), the portion of the aircraft noise footprint of particular interest in the flyover and sideline planes lies between a θ of 60° and 120°. The flyover and sideline overall sound pressure level measurements presented herein include this range of interest. In order to show the spectral detail of the noise, and yet limit the number of plots, only data at a θ of 70° and 100° are presented for the flyover and sideline planes. The data at these angles are representative of that in the forward (θ, 20° to 90°) and aft (θ, 90° to 120°) quadrants below the configurations. Although measurements were made at jet Mach numbers of 0.5, 0.7, and 0.8, only the results at 0.7 are presented herein as typical data. Acoustic data are presented for configuration 1 at an X/D of 2 and 4; for configurations 2 and 3 at an X/D of 2, 4, and 7.33; for configuration 4 at an X/D of 2; and for configurations 5 and 6 at an X/D of 2 and 4. (The overall sound pressure level test results presented for configurations 1, 2, and 3 were published previously in ref. 17.)

Free-field perceived noise level data scaled to full size are presented only for configuration 3 because the scaling laws for the externally blown flap in the approach attitude are not as yet firmly known (ref. 18); thus the reliability of scaled data is questionable. These data are presented only to demonstrate in a very general sense the magnitude of the full scale suppression of jet-flap interaction noise, which may be achieved by using the suppression devices described in this study.

Measured aerodynamic performance characteristics are presented in table I for each configuration in the form of a dimensionless lift coefficient F_N/T, a dimensionless thrust coefficient F_a/T, flow turning efficiency η, and the flow turning angle. The thrust T represents the calculated ideal nozzle thrust using an ideal mass flow rate for a nozzle having a diameter of 5.08 centimeters. The flow turning angles are referenced to the downstream nozzle centerline axis. Aerodynamic performance data are presented for all configurations at an X/D of 2, 4, and 7.33.

Results and Discussion

Measured noise data for the six configurations considered here are presented graphically in figures 9 to 21. For each configuration the overall sound pressure level directivity and spectra are presented in the flyover and sideline planes. The overall sound pressure level data

TABLE I. - AERODYNAMIC PERFORMANCE CHARACTERISTICS OF EBF CONFIGURATION AT A JET MACH NUMBER OF 0.7

Configuration	Separation distance, X/D	Thrust coefficient, F_a/T	Lift coefficient, F_N/T	Turning efficiency, η	Turning angle, deg
Reference	7.33	0.33	0.53	0.62	58.1
1 (Unsuppressed)	4	0.38	0.53	0.65	54.4
	2	0.36	0.55	0.66	56.8
2 (Plugs in slots)	7.33	0.36	0.48	0.60	53.1
	4	0.36	0.46	0.58	52
	2	0.36	0.47	0.60	52.5
3 (Plugs in slots with ramped screen (h = 1.27 cm))	7.33	0.28	0.44	0.52	57.5
	4	0.27	0.43	0.51	57.9
	2	0.28	0.44	0.52	57.5
4 (Screens over slots)	7.33	0.37	0.51	0.63	54.0
	4	0.38	0.52	0.64	53.8
	2	0.32	0.51	0.60	57.9
5 (Ramped screen (h = 1.27 cm))	7.33	0.33	0.46	0.57	54.3
	4	0.30	0.48	0.57	58
	2	0.33	0.51	0.61	57.1
6 (Screens over slots with ramped screen)	7.33	0.29	0.47	0.55	58.3
	4	0.32	0.50	0.59	57.4
	2	0.31	0.46	0.55	56

are presented between radiation angles θ of 20° and 120°, and the spectra for θ of 70° and 110°.

In order to aid in the discussion of these data, tables II and III list average sound level attenuations or amplifications for each configuration. The attenuations or amplifications represent the difference between the sound pressure level produced by the reference configuration and a particular test configuration. For the discussions of the spectral data appearing in table III, it will be more convenient to refer to specific frequency ranges as: very low (200 to 800 Hz), low (1.25 to 2.5 kHz), mid (3.15 to 8 kHz), high (10 to 20 kHz) and very high (31.5 to 63 kHz). In the following discussion, the reader is referred principally to these tables. Reference to the graphical data on the appropriate figure, noted in the tables, may be made as desired.

The following discussion of the experimental results is divided into five parts. First, the noise attenuations and amplifications in tables II and III are discussed for the unsuppressed configuration (configuration 1) at reduced nozzle to flap separation distances X/D of 2 and 4. Both the overall sound pressure level directivity data (table II) and the spectral data (table III) in the low through the very high frequency ranges relevant to aircraft noise abatement are considered. In addition, a comparison is made between the static aerodynamic performance characteristics of the unsuppressed configuration and the reference configuration. Following this, a similar presentation is made for each of the other five configurations equipped with suppression devices (suppressed configurations). Second, a discussion of the very low frequency acoustic data (table III), which contribute to the production of cabin noise and structural vibration, is presented for all the configurations. Third, a comparison is made of the noise and static aerodynamic performance characteristics produced by configurations 2 and 3 positioned at nozzle-to-flap separation distances of 7.33 and 2 nozzle diameters. Fourth, a qualitative estimate of the noise suppression and aerodynamic performance characteristics of the suppression devices used alone or in combination is made as a function of separation distance using tables III and I, respectively. Finally, some concluding remarks are made about the experimental results.

TABLE II. - AVERAGE OVERALL SOUND PRESSURE (OASPL) ATTENUATION (+) OR AMPLIFICATION (-) IN dB RELATIVE TO REFERENCE CONFIGURATION

Configuration	Separation distance, X/D	Directivity angle, deg									Figure
		Forward quadrant					Aft quadrant				
		40	50	60	70	80	90	100	110	120	
		Change in OASPL, dB (re 20 $\mu N/m^2$)									
(a) Flyover plane ($\varphi = 90^o$)											
Reference	7.33	0	0	0	0	0	0	0	0	0	9(a)
1 (Unsuppressed)	4	-3	-0.8	-0.2	-0.7	-0.7	0.6	0.5	1.5	4.2	9(a)
	2	-2.2	-1.5	-1.5	-1.3	-0.7	0	-1.5	0.7	5.1	9(a)
2 (Plugs in slots)	7.33	4.1	6	6	5.3	4.5	4.8	3.1	1	-2.2	11(a)
	4	2	3.6	4.1	3.3	3	2.6	1	0.7	1.2	11(a)
	2	2	3	3.2	2.6	2.1	0.6	-1.9	-1	0.6	11(a)
3 (Plugs in slots with ramped screen (h = 1.27 cm))	7.33	5.5	7.3	7.2	5.1	2.7	2.1	3.4	5.7	3.6	13(a)
	4	4.2	5.5	5.4	5.1	2	2.3	4	6.1	10	13(a)
	2	5.3	6.7	6.1	4.6	3	3.6	5.5	9.2	10.5	13(a)
4 (Screens over slots)	2	-0.5	----	----	0.7	----	1	-0.2	1.1	----	16(a)
5 (Ramped screen (h = 1.27 cm))	4	-0.5	-0.2	0	-0.7	-1.5	0	1.3	5.6	8.5	18(a)
	2	-2.2	----	----	0	----	1.4	1.9	5.6	----	18(a)
6 (Screens over slots with ramped screen)	4	0.5	2.2	2.3	1	0	1	2.5	5.7	9.8	20(a)
	2	2.5	3.7	3.5	2.4	2.2	2.4	3.5	10.3	----	20(a)
(b) Sideline plane ($\varphi = 22^o$)											
Reference	7.33	0	0	0	0	0	0	0	0	0	10(a)
1 (Unsuppressed)	4	-1	-1	0.1	-0.5	1	2.1	1.5	1.6	1.8	10(a)
	2	-1.5	-1.6	-2.2	-3	-1.1	0.6	0	-1	-1.7	10(a)
2 (Plug in slots)	7.33	3.5	2.9	2.5	1.6	1.7	3.6	1.9	1.7	2.5	12(a)
	4	1	0.7	0.6	-0.2	0.8	3.2	3.5	2.6	2	12(a)
	2	0.7	0.4	0.3	0.2	1.3	3.5	2	1.3	0	12(a)
3 (Plugs in slots with ramped screen (h = 1.27 cm))	7.33	3	3	2.3	1.5	2	2.5	2.1	2.2	3.9	14(a)
	4	1.6	1.5	0.6	-1	1	3.5	3.2	3.1	3.9	14(a)
	2	3.9	1.5	1	0	1.2	5.1	3	3.7	4.2	14(a)
4 (Screens over slots)	2	-0.5	----	----	-1.5	----	2.5	1.7	0.5	0	17(a)
5 (Ramped screen (h = 1.27 cm))	4	-0.6	-0.4	0.1	-0.5	1.2	3	1.7	1.9	2.4	19(a)
	2	0.7	----	----	-3	----	1.9	1.4	1.1	0.2	19(a)
6 (Screens over slots with ramped screen)	4	2.5	0.5	1.2	0.6	2.6	4.6	2.7	2.8	4.6	21(a)
	2	1.1	0.5	0.6	-1.3	2	3.5	3.1	3.5	8.2	21(a)

TABLE III. - AVERAGE SOUND PRESSURE LEVEL (SPL) ATTENUATION (+) OR AMPLIFICATION (-)

RELATIVE TO REFERENCE CONFIGURATION

(a) Flyover plane ($\varphi = 90^{o}$)

Configuration	Quadrant	Directivity angle, θ, deg	Separation distance, X/D	Frequency range, kHz					Figure
				Very low	Low	Mid	High	Very high	
				0.2 to 0.8	1.25 to 2.5	3.15 to 8	10 to 20	31.5 to 63	
				Change in SPL, dB (re 20 $\mu N/m^2$)					
Reference	Forward	70	7.33	0	0	0	0	0	9(b)
	Aft	110	7.33	0	0	0	0	0	9(c)
1 (Unsuppressed)	Forward	70	4	4.0	0	-1.3	-1	-2.4	9(b)
		70	2	7.2	0	-2.7	-2.2	-3.1	9(b)
	Aft	110	4	3.4	1	1.5	0	-2	9(c)
		110	2	5	1	1	-0.5	-1.6	9(c)
2 (Plugs in slots)	Forward	70	7.33	2.8	5.5	5.6	4.5	1.2	11(b)
		70	4	4.2	4.4	3.5	2.1	-2.2	11(b)
		70	2	7.5	3	2	2.1	-1.7	11(b)
	Aft	110	7.33	5.1	1.8	-1	1.5	2.5	11(c)
		110	4	5	0	-0.5	0.5	-1.5	11(c)
		110	2	8.5	0	-3.1	0	-2	11(c)
3 (Plugs in slots with ramped screen (h = 1.27 cm))	Forward	70	7.33	3.7	7.2	5.3	2.5	-1.7	13(b)
		70	4	4	5.5	3.2	0	-5	13(b)
		70	2	8.5	6	4.5	3	-4	13(b)
	Aft	110	7.33	5.2	5.7	2.8	2.4	1	13(c)
		110	4	6.2	7	3.5	1	-2	13(c)
		110	2	10	11	8.2	3.7	-4	13(c)
4 (Screens over slots)	Forward	70	2	8.9	1.8	0.75	-1	-6	16(b)
	Aft	110	2	7.5	1.5	1.5	0.25	-2.4	16(c)
5 (Ramped screen (h = 1.27 cm))	Forward	70	4	4	0	-1.5	-2	-4	18(b)
		70	2	8.7	2.7	-2	-3.1	-7.5	18(b)
	Aft	110	4	4.7	6	3	0	-2.0	18(c)
		110	2	8.1	9	11	7.7	3.2	18(c)
6 (Screens over slots with ramped screen)	Forward	70	4	5.4	2.0	1.5	-2.2	-6.5	20(b)
		70	2	9.2	4.5	1.5	-0.5	-5	20(b)
	Aft	110	4	6	6.5	3.7	-1.5	-3.3	20(c)
		110	2	9	9.5	11.2	6.5	3.4	20(c)

TABLE III. - Concluded.

(b) Sideline plane ($\varphi = 22^{o}$)

Configuration	Quadrant	Directivity angle, θ, deg	Separation distance, X/D	Frequency range, kHz					Figure
				Very low	Low	Mid	High	Very high	
				0.2 to 0.8	1.25 to 2.5	3.15 to 8	10 to 20	31.5 to 63	
				Change in SPL, dB (re $20\mu N/m^2$)					
Reference	Forward	70	7.33	0	0	0	0	0	10(b)
	Aft	110	7.33	0	0	0	0	0	10(c)
1 (Unsuppressed)	Forward	70	4	3.5	0	-1.5	-1	-3	10(b)
		70	2	7.8	0	-7.3	-5.5	-3.7	10(b)
	Aft	110	4	4.5	1	1.9	2.5	0	10(c)
		110	2	5	-2.5	0	4.1	5	10(c)
2 (Plugs in slots)	Forward	70	7.33	3	3	0	-1	-3	12(b)
		70	4	3.2	1	-2.8	-2.5	-3.4	12(b)
		70	2	9.5	4	-3	-2.5	-3.2	12(b)
	Aft	110	7.33	1.5	3	3	2.5	0	12(c)
		110	4	2.7	1.5	7	7.2	7.4	12(c)
		110	2	5.8	0	2.5	7	6.4	12(c)
3 (Plugs in slots with ramped screen (h = 1.27 cm))	Forward	70	7.33	3.2	4	0	-3	-4.1	14(b)
		70	4	4	2.5	-3.0	-4.5	-6	14(b)
		70	2	8.5	5.5	-2.4	-2	-3.5	14(b)
	Aft	110	7.33	1.5	3.5	2	1.5	0.5	14(c)
		110	4	2.2	2.4	7.5	7.3	5.5	14(c)
		110	2	7	3.0	5.0	9	7	14(c)
4 (Screens over slots)	Forward	70	2	8.7	2.5	-4.5	-7	-7.5	17(b)
	Aft	110	2	6	-1.5	2.5	4	3	17(c)
5 (Ramped screen (h = 1.27 cm))	Forward	70	4	3.5	0.5	-1.5	-3.5	-5	19(b)
		70	2	8.2	1.5	-7.1	-6.5	-7.5	19(b)
	Aft	110	4	3.7	0.7	2	2.3	0.7	19(c)
		110	2	6	-0.5	0.7	3	2	19(c)
6 (Screens over slots with ramped screen)	Forward	70	4	4.5	3.5	-2	-3.5	-6.5	21(b)
		70	2	9	3.5	-2.7	-8	-8	21(b)
	Aft	110	4	4.8	3	3.5	3	-0.5	21(c)
		110	2	7	2	3.5	5	2.3	21(c)

Configuration 1 at Reduced Separation Distances

OASPL.—With an exception at a θ of 120°, the data indicate that only small changes occurred in the overall sound pressure level of the noise produced by configuration 1 at reduced nozzle-to-flap separation distances of 2 and 4 in the flyover and sideline planes compared with that for the reference configuration. The peak noise produced by both configurations occurred at a θ of 60° in the flyover plane and at a θ of 40° in the sideline plane as shown in figures 9(a), and 10(a), respectively. This lack of change in the peak noise angle indicates that the same sound sources are present in both configurations.

Spectra.—A more detailed description of the acoustic effects is provided from a consideration of the spectra. The spectral data indicate that the small amplifications in

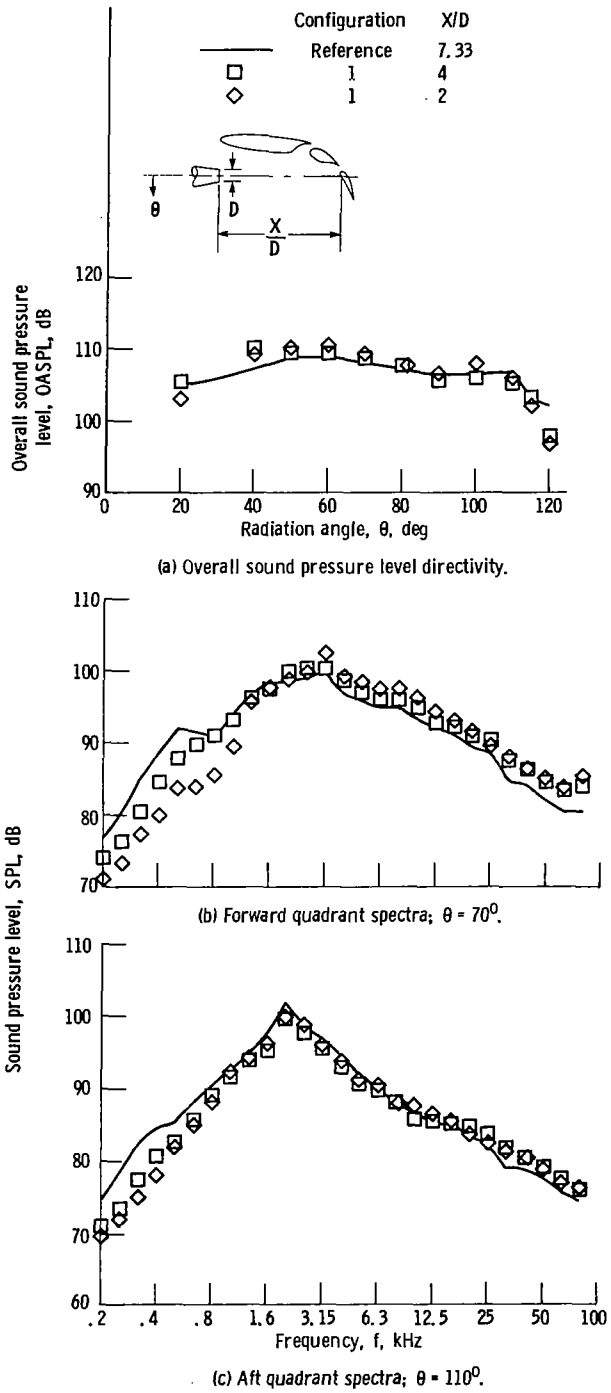

Figure 9. - Comparison of free-field acoustic data for reference configuration and unsuppressed configuration (configuration 1) in flyover plane (φ = 90°).

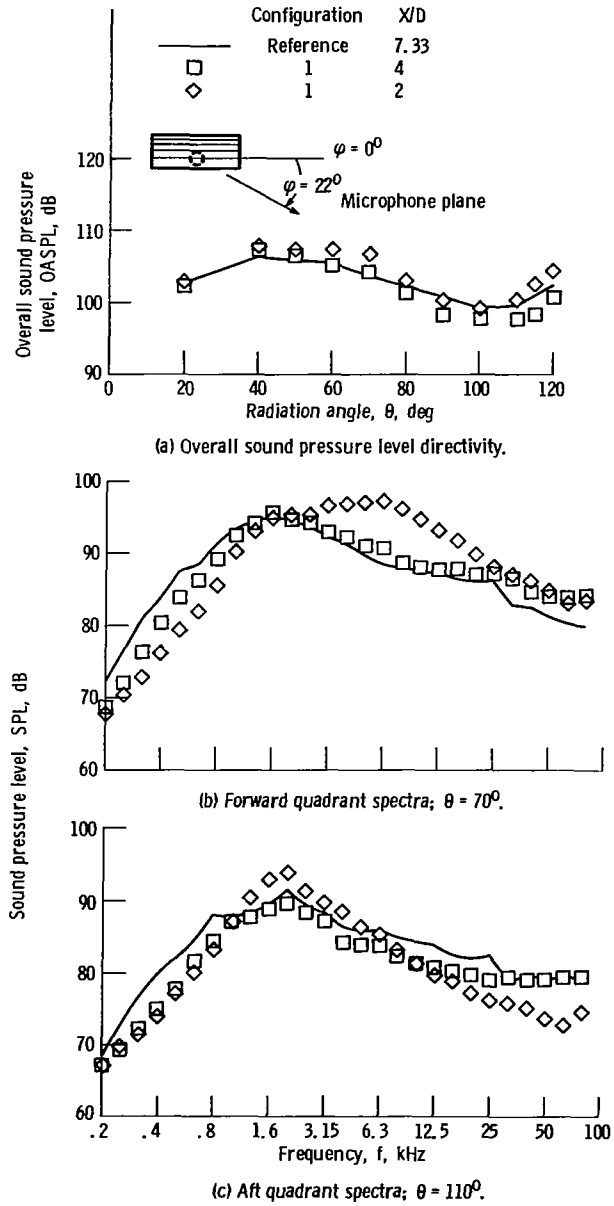

Figure 10. - Comparison of free-field acoustic data for reference configuration and unsuppressed configuration (configuration 1) in sideline plane (φ = 22°).

overall sound pressure level for configuration 1 are, in general, the result of increased sound pressure levels in the mid-frequency range near the spectral peaks. These increased levels are due to a difference in the jet centerline velocity at the location of the flaps between configuration 1 and the reference configuration. For configuration 1, there is a 10 percent increase in the jet centerline velocity (ref. 19) at an X/D of 2 and 4 compared with that for the reference configuration (X/D of 7.33). This 10 percent increase in jet centerline velocity should produce a nominal increase in the noise produced by configuration 1 of 3 dB, based on a 6 power dependence of the velocity. In addition to these small mid-frequency amplifications, a large amplification (7 dB) of the mid-frequency sound levels occurred at an X/D of 2 in the forward quadrant of the sideline plane (fig. 10(b)). This amplification was due to a large shift upward in the frequency of the spectral peak in comparison to the reference configuration. At this time, no explanation for this shift exists. In contrast to these amplifications, attenuations of high- and very high-frequency broadband sound levels of up to 5 dB occurred at X/D of 2 in the aft quadrant of the sideline plane. This demonstrates that significant mid- through very high-frequency broadband attenuations can occur simply by reducing the separation distance between the nozzle exit plane and the second flap of the UTW EBF configuration in its approach attitude.

The high-frequency attentuations that occurred in the aft quadrant of the sideline plane at an X/D of 2 are of special interest in a propulsion system design study, such as that of reference 5. Reference 5 indicates that the engine noise peaks at a radiation angle of 120° in the aft quadrant of the sideline plane (φ of 22°). Therefore, it concludes that the suppression of jet-flap interaction noise at this location is important in order to achieve a balanced propulsion system design. The suppression capability demonstrated here of the higher frequency noise in the aft quadrant of the sideline plane is, therefore, considered important in order to achieve a balanced acoustic design. These data demonstrate how a specific noise suppression technique applied to a wing-flap system can be used to beneficially tailor the noise characteristics of a propulsive lift concept.

Performance.—The dimensionless thrust and lift coefficients of configuration 1 presented in table I were larger than those of the reference configuration by nominally 0.04 (12%) and 0.01 (2%), respectively. These resulted in a 0.03 (6%) increase in turning efficiency and a 2.5° increase in the flow turning angle.

Configuration 2 at Reduced Separation Distances

OASPL.—The data in table II representing the differences between configuration 2 at the reduced separation distances and the reference configuration indicate that with the exception of the aft quadrant in the flyover plane significant overall sound pressure level attenuations of up to 4 dB occurred. The peak overall sound pressure level in the flyover plane (fig. 11(a)) occurred at a θ of approximately 100°, unlike configuration 1 and the reference configuration. This indicates that a change has occurred in the noise sources

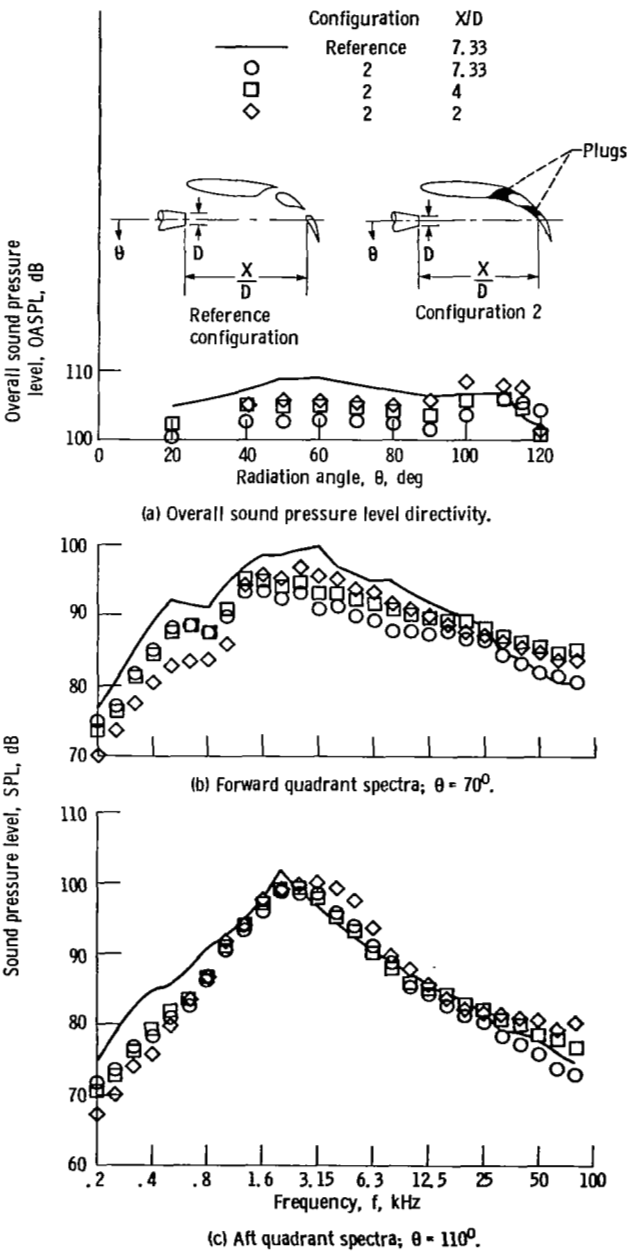

Figure 11. - Comparison of free-field acoustic data for reference configuration and configuration with plugs in slots (configuration 2) in flyover plane (φ = 90°).

in relation to the reference configuration. The peak overall sound pressure level in the sideline plane (fig. 12(a)) occurred at a θ of 40°, as in the case of configuration 1 and the reference configuration.

Spectra.—The experimental results in table III indicate that the plugs of configuration 2 produced moderate low- and mid-frequency noise attenuations of 4 dB in the forward quadrant of the flyover plane. In the aft quadrant of the sideline plane at an X/D of 2 and 4, larger broadband mid- through very high-frequency attenuations of 7 dB also occurred. The large high-frequency attenuations were independent of separation distance and will result in meaningful reductions of perceived noise levels (PNL), which are important for a propulsion system design study where the engine noise peaks in the aft quadrant of the sideline plane, as previously discussed. In contrast to these attenuations configuration 2 produced small noise amplifications in the aft quadrant of the flyover plane and in the forward quadrant of the sideline plane.

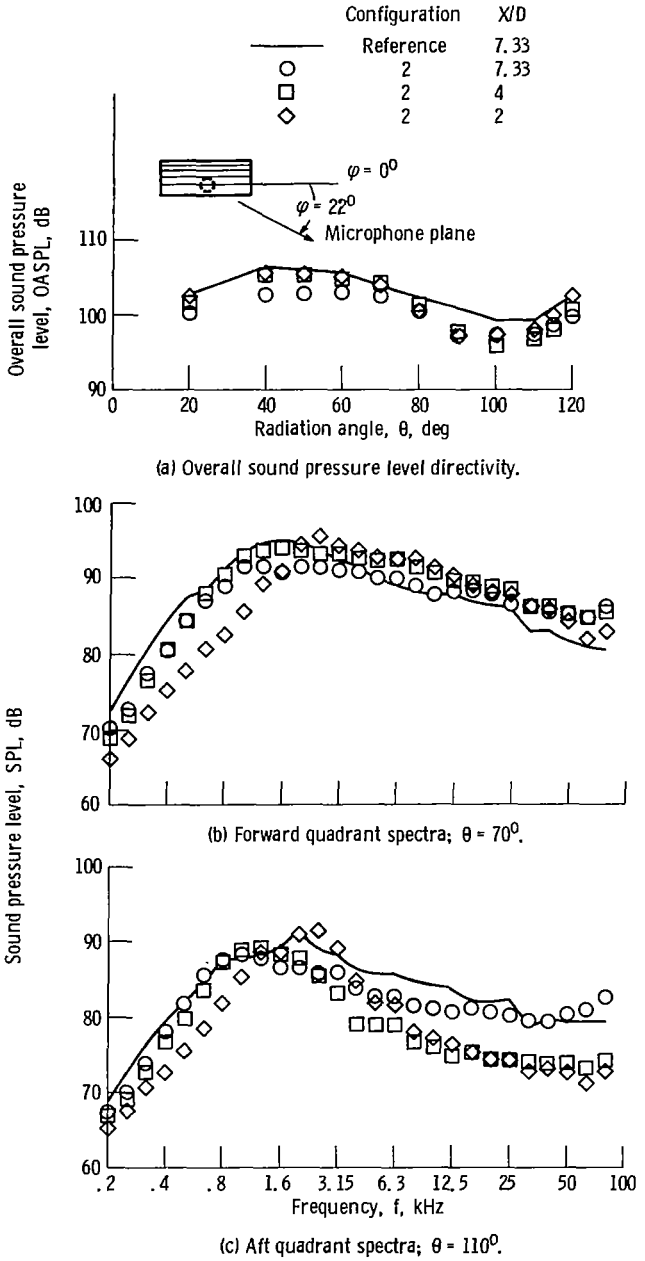

Figure 12. - Comparison of free-field acoustic data for reference configuration and configuration with plugs in slots (configuration 2) in sideline plane ($\varphi = 22^0$).

Performance.—Table I indicates that configuration 2 produced an increase above the reference configuration of 0.03 (9%) in the dimensionless thrust coefficient with a decrease of 0.06 (12%) in the dimensionless lift coefficient. These had the net effect of reducing the flow turning efficiency below the reference configuration by 0.03 (5%) and the flow turning angle by 6°.

Configuration 3 at Reduced Separation Distance

OSAPL.—Large overall sound pressure level attenuations up to 10.5 dB and 4 dB occurred throughout the entire range of radiation angles in both the flyover and sideline planes, respectively, for configuration 3 (table II). The peak overall sound pressure levels occurred at a θ of 80° and 60° in the flyover (fig. 13(a)) and sideline (fig. 14(a)) planes, respectively, unlike the reference configuration where the noise peaked at a θ of 60° and 40° in the flyover and sideline planes, respectively. Thus, a change has occurred in the noise sources throughout the entire measured noise field in relation to the reference configuration.

Spectra.—The spectral data indicate that the plugs and ramped screen used in configuration 3 at an X/D of 2 and 4 have, in general, produced moderate to large low- through high-frequency noise attenuations throughout the flyover plane and in the aft quadrant of the sideline plane. These attenuations are larger than those produced by configurations 1 or 2. Several of the largest attenuations include broadband low-frequency attenuations of 11 and 7 dB in the aft quadrant of the flyover plane at separation distances of 2 and 4 nozzle diameters, respectively, and high-frequency attenuations of 9 and 7 dB, respectively, in the aft quadrant of the sideline plane. Conversely, the only significant broadband amplifications (up to 6 dB) occurred at an X/D of 4 in the very high-frequency range in the forward quadrant of the sideline plane.

PNL.—The noise reductions produced by configuration 3 clearly represent meaningful reductions in perceived noise levels (PNL). Scaled free-field perceived noise level calculations representing the jet-flap impingement noise produced by the reference configuration and configuration 3 at an X/D of 2 are compared in figure 15.

The calculations were made by performing a constant

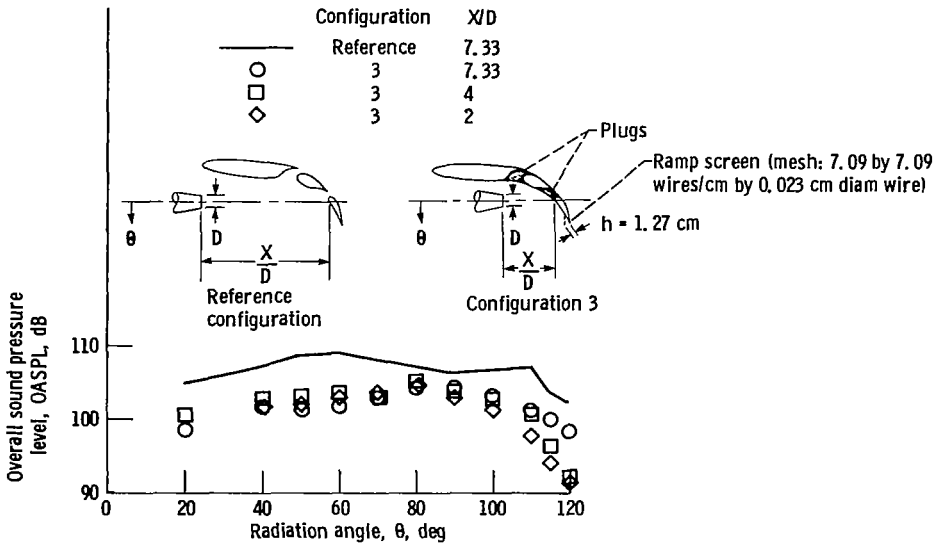

(a) Overall sound pressure level directivity.

(b) Forward quadrant spectra; $\theta = 70^{o}$.

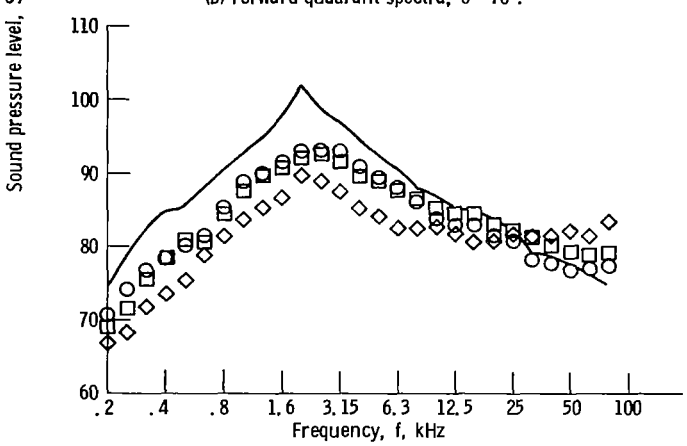

(c) Aft quadrant spectra; $\theta = 110^{o}$.

Figure 13. - Comparison of free-field acoustic data for reference configuration and configuration with plugs in slots and ramped screen (configuration 3) in flyover plane ($\varphi = 90^{o}$).

Strouhal number frequency shift on the measured data of figures 13 and 14 and adjusting the amplitude in proportion to the square of the scale change of the nozzle exit diameter. Temperature effects were neglected. The correctness of this scaling procedure in the case of the EBF in the approach attitude is not certain since a number of sources are responsible for the noise, all of which may not scale similarly (ref. 8). Nevertheless, these calculations are performed to demonstrate the approximate suppression of jet-flap interaction noise to be expected by using the devices described herein. A diameter of 0.66 meter (26 in.) was chosen as representative of a full scale nozzle exit diameter. Free-field perceived noise levels are presented in figures 15(a)

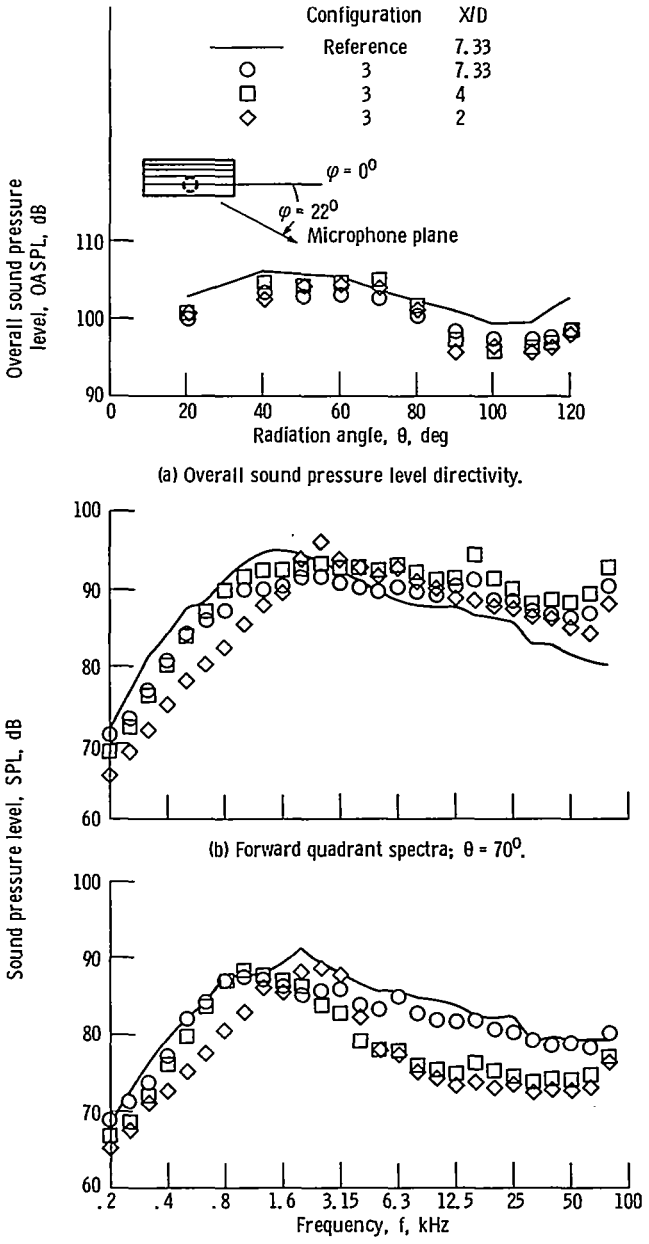

(a) Overall sound pressure level directivity.

(b) Forward quadrant spectra; $\theta = 70^0$.

(c) Aft quadrant spectra; $\theta = 110^0$.

Figure 14. - Comparison of free-field acoustic data for reference configuration and configuration with plugs in slots and ramped screen (configuration 3) in sideline plane ($\varphi = 22^0$).

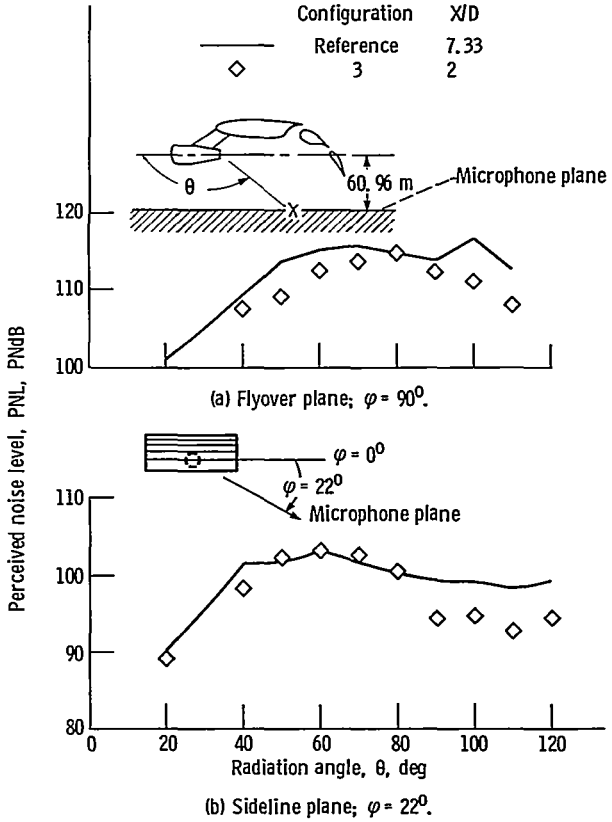

(a) Flyover plane; $\varphi = 90^0$.

(b) Sideline plane; $\varphi = 22^0$.

Figure 15. - Comparison of free-field perceived noise level for reference configuration and configuration with plugs in slots and ramped screen (configuration 3). Aircraft at 60.96 meters altitude. $M_j = 0.7$; nozzle diameter D = 0.66 meter; four engines.

and (b) representing the flyover and sideline planes, respectively, for a four-engine aircraft operating at an altitude of 61 meters (200 ft) and the observer located at a sideline distance of 152 meters (500 ft). In the forward quadrant between a θ of 40° and 90° in the flyover plane, noise attenuations of nominally 2 PNdB occurred; and in the aft quadrant between a θ of 100° and 110°, attenuations of 5 PNdB occurred. In the forward quadrant between a θ of 20° and 80° in the sideline plane, small attenuations of nominally 1 PNdB occurred; and in the aft quadrant between a θ of 90° and 120°, attenuations of nominally 5 PNdB occurred.

Performance.—Although configuration 3 produced large attenuations of the interaction noise, these were accompanied by a 0.05 (17%) and 0.09 (17%) reduction in the dimensionless, thrust and lift coefficients, respectively. These produced a 0.10 (17%) reduction in flow turning efficiency with a negligible reduction in flow turning angle.

Configuration 4 at Reduced Separation Distance

With forward speed (in flight), a detached flow problem on the upper surface of the flaps may develop for configurations 2 and 3. In these configurations the first and second flaps are positioned at 30° and 60°, respectively, in relation to the wing, as shown in figure 2. With the slots between the wings and flaps partially covered by the plugs, shown in figures 6 and 7, it is clearly possible that the flow passing over the upper surface of the flaps during flight may become unstable or detach entirely. In this regard, the forward flight wind tunnel test results reported in reference 6 are of interest. The results of reference 6 suggest that the use of a single plug fairing in the slot between the two flaps of either configuration 2 or 3 would not produce flow separation. Should free stream flow separation become a problem

during flight, it may only be necessary to allow a relatively small amount of air to flow through the slot between the wing and first flap to rectify the problem. Such a procedure should affect only slightly the noise suppression effectiveness and/or the aerodynamic performance.

In the present study, configurations 4 and 5 were designed specifically to permit partial flow through the flap openings. Screens were substituted in place of the plug fairings so that a small controlled amount of flow could pass over the upper surfaces of the flaps thereby establishing a boundary layer, which in turn would promote attached flow in flight.

Attenuation (or amplification) data produced by configuration 4 are presented at a single nozzle-to-flap separation distance X/D of 2 and at a limited number of radiation angles θ of 40°, 70°, 90°, 100°, and 110°.

OASPL.—With exceptions in the aft quadrant of the sideline plane, small attenuations of the overall sound pressure level occurred throughout the sound field of

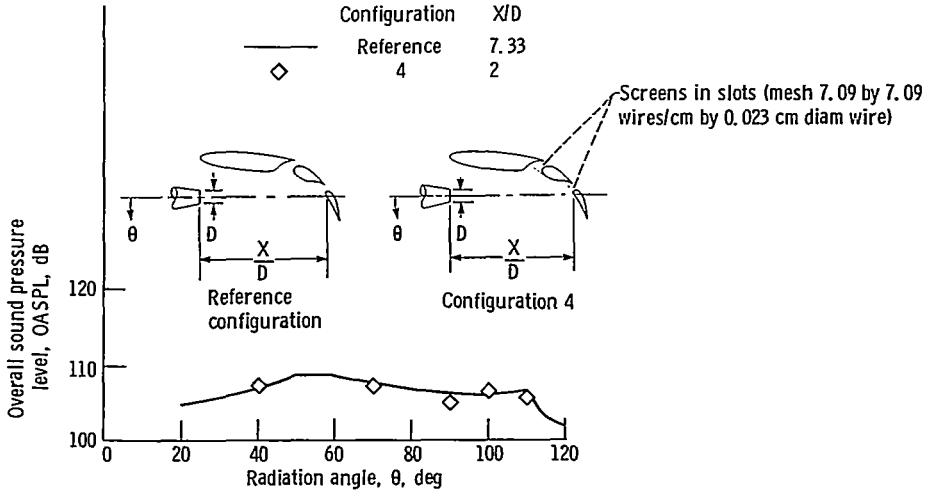

(a) Overall sound pressure level directivity.

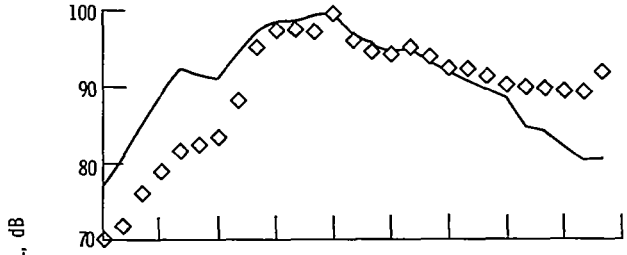

(b) Forward quadrant spectra; $\theta = 70^0$.

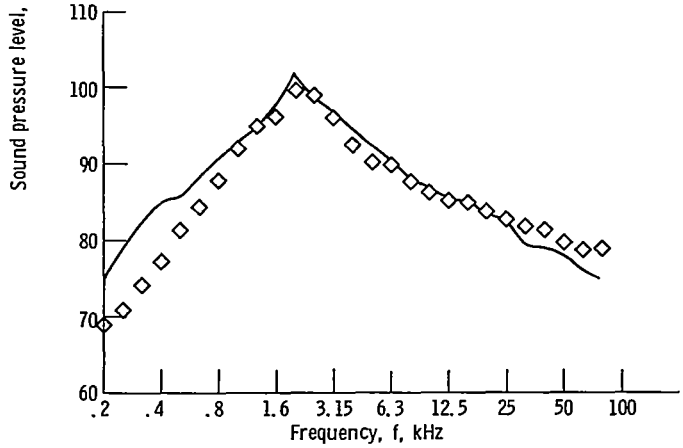

(c) Aft quadrant spectra; $\theta = 110^0$.

Figure 16. - Comparison of free-field acoustic data for reference configuration and configuration with screens over slots (configuration 4) in flyover plane ($\varphi = 90^0$).

configuration 4 in comparison to the reference configuration. In the aft quadrant of the sideline plane attenuations up to 2.5 dB occurred. The peak sound level appears to occur at the same radiation angles in the flyover (fig. 16(a)) and sideline (fig. 17(a)) planes as the reference configuration, indicating that the same sound sources are present in both configurations.

Spectra.—Configuration 4 produced significant noise attenuations only in the aft quadrant of the sideline plane where a nominal 3 dB attenuation of the mid- through very high-frequency noise occurred. Conversely, in the forward quadrant of the flyover and sideline planes, very high-frequency noise amplification of nominally 6 dB were generated. The amplifications produced in the forward quadrant of the sideline plane were similar to those produced by configuration 1 and were the result of an unusually large shift upward in the frequency of the spectral peak in comparison to the reference configuration (fig. 17 (b)).

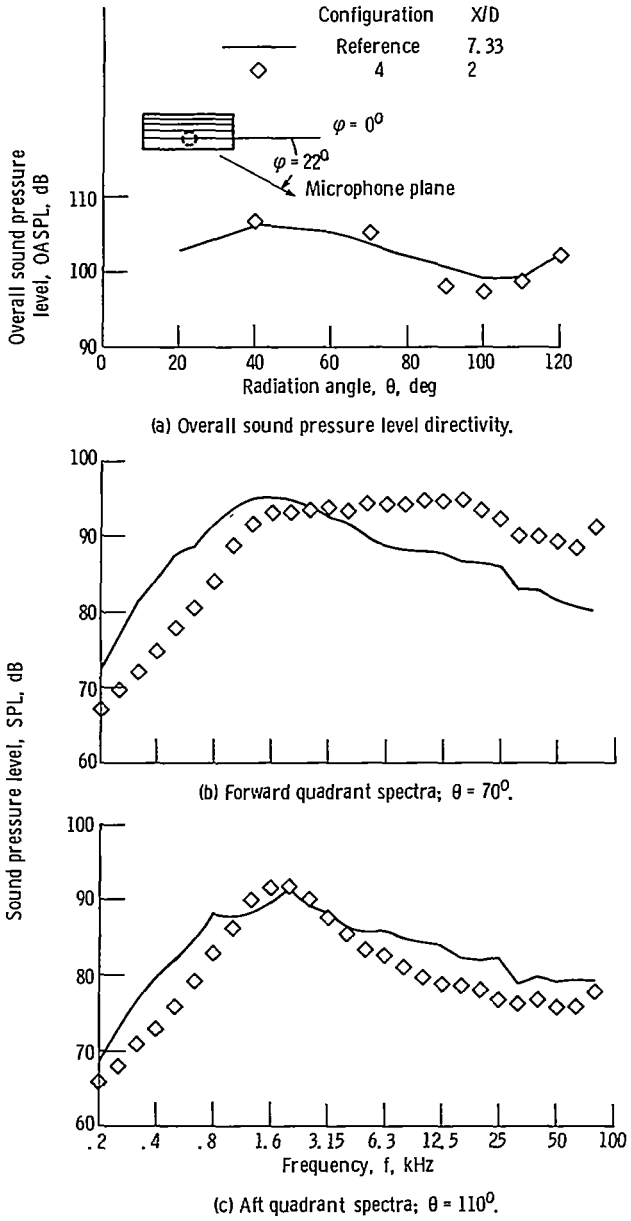

Figure 17. - Comparison of free-field acoustic data for reference configuration and configuration with screens over slots (configuration 4) in sideline ($\varphi = 22^0$).

It should be emphasized that in the aft quadrant of the flyover plane, only small differences existed between the noise produced by configurations 2 and 4 at a reduced separation distance of 2 nozzle diameters (table III). This indicates that neither the plugs of configuration 2 nor the screens of configuration 4 were effective in reducing the noise produced in this quadrant of the flyover plane; and, it implies that at least two independent noise sources are acting in the flyover plane of configuration 1. Several other comparisons between configurations indicate that: first, more high- and very high-frequency noise was produced by the screens of configuration 4 in the forward quadrants of both the flyover and sideline planes than configuration 1 or the plugs of configuration 2; and second, in the very low-frequency range the noise reductions produced by configurations 2 and 4 at an X/D of 2 were essentially the same, thus, indicating that these reductions were independent of the differences between the suppression devices.

Performance.—From table I, the acoustic effects were accompanied by an increase in the average thrust coefficient of 0.02 (6%) above the reference configuration and a decrease in the average lift coefficient of 0.02 (4%). These produced no change in the average flow turning efficiency, but a 2° reduction in the average flow turning angle. Thus, where suppression of the noise below the reference configuration occurred, the screens of configuration 4 acted in a similar way to the nonporous plugs used in configuration 2.

Configuration 5 at Reduced Separation Distances

OASPL.—Nominally no attenuations or amplifications occurred in the forward quadrants of the flyover and sideline planes (table II) with configuration 5. However, in the aft quadrants of the flyover and sideline planes attenuations amounting to as much as 8.5 and 3 dB were produced, respectively. The peak overall sound pressure level occurred at the same radiation angles in the flyover (fig. 18(a)) and sideline (fig. 19(a)) planes as the reference configuration indicating that the same sound sources were present in both configurations.

Spectra.—At separation distances of 2 and 4 nozzle diameters in the aft quadrant of the flyover plane, configuration 5 produced large low- to high-frequency attenuations up to 11 and 6 dB, respectively. In the aft quadrant of the sideline plane small attenuations occurred. In contrast, a broad range of mid- to very high-frequency amplifications up to 7 dB were produced in the forward quadrants of both the flyover and sideline

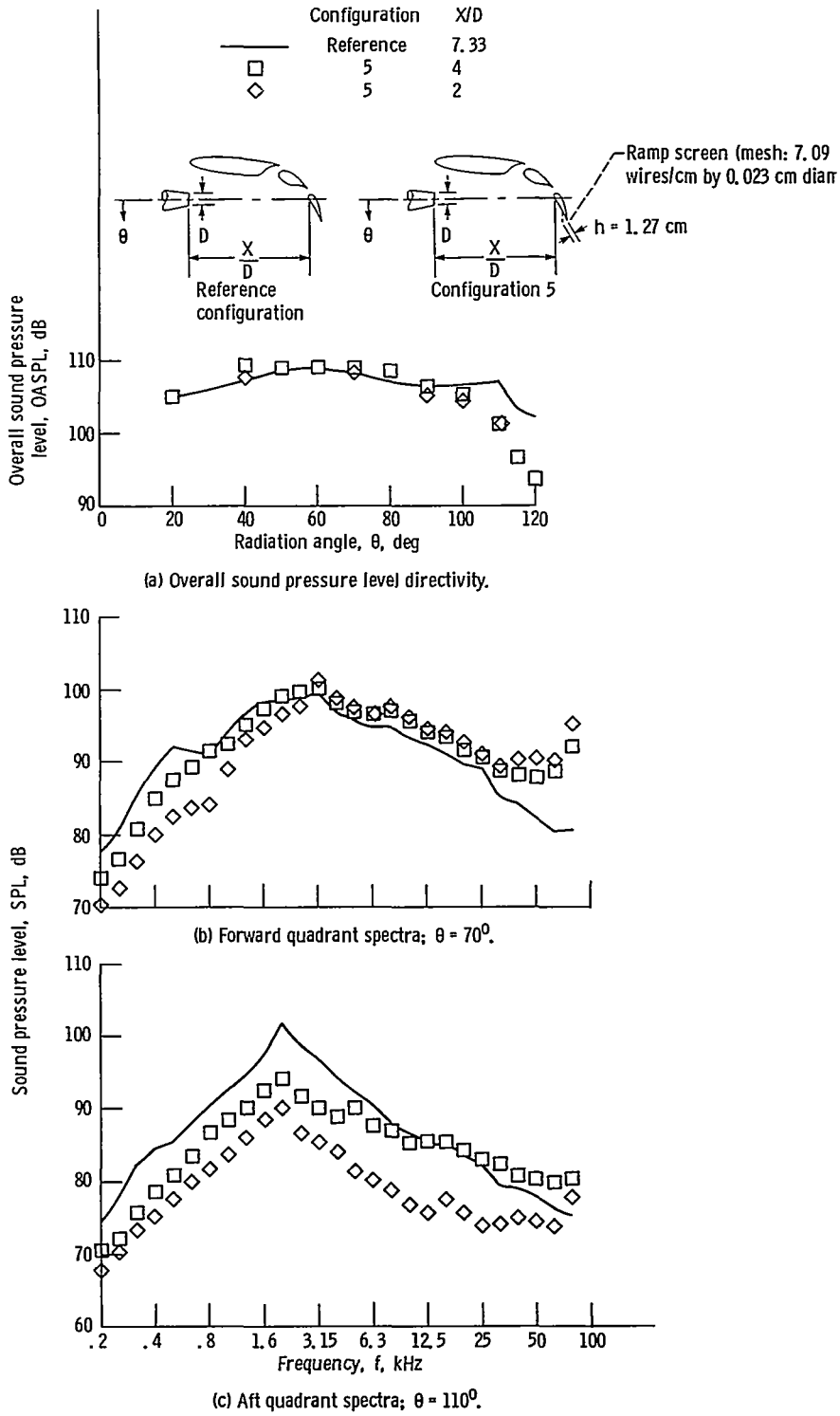

Figure 18. - Comparison of free-field acoustic data for reference configuration and configuration with ramped screen (configuration 5) in flyover plane ($\varphi = 90^0$).

planes. In the sideline plane, these amplifications were due to an unusually large increase in the frequency at which the spectral peaks occurred (fig. 19(b)). The largest amplifications occurred at a separation distance of 2 nozzle diameters. Thus, the ramped screen of configuration 5 produced a highly selective, but significant, attenuation in the aft quadrant of the flyover plane.

Performance.—In relation to the reference configuration, configuration 5 produced an average

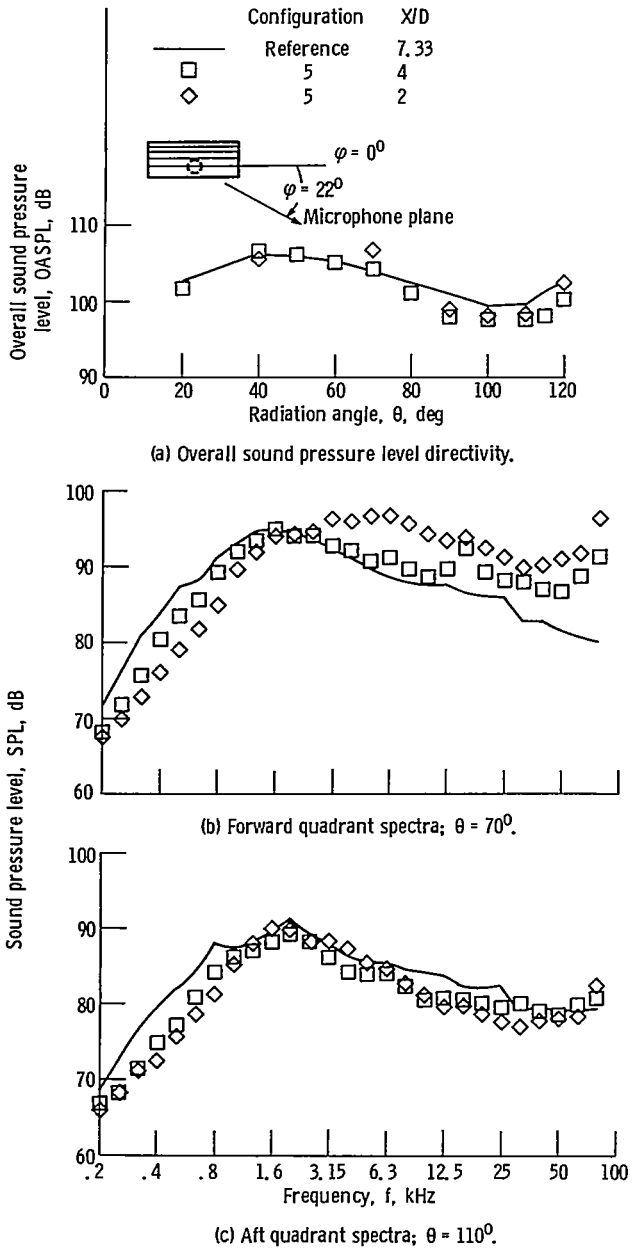

Figure 19. - Comparison of free-field acoustic data for reference configuration and configuration with ramped screen (configuration 5) in sideline plane ($\varphi = 22^0$).

decrease in the dimensionless thrust and lift coefficients of 0.02 (5%) and 0.04 (7%), respectively, resulting in an average decrease of 0.03 (5%) in the flow turning efficiency and a 0.5° decrease in the flow turning angle.

Configuration 6 at Reduced Separation Distances

OASPL.—Reductions in the nozzle-to-flap separation distance of configuration 6 produced overall sound pressure level attenuations (table II) throughout the entire range of radiation angles in both the flyover and sideline planes. These attenuations reached nominally 9 dB at a θ of 120° in the flyover and sideline planes. And the peak sound level occurred at a θ of 70° and 50° in the flyover (fig. 20(a)) and sideline (fig. 21(a)) planes, respectively, unlike the reference configuration where the noise peaked at a θ of 60° and 40° in the flyover and sideline planes, respectively. Thus, a change occurred in the noise sources throughout the entire measured noise field in relation to the reference configuration.

Spectra.—The screens of configuration 6 produced large broadband attenuations in the aft quadrant of the flyover plane at an X/D of 2 which varied up to 11 and 7 dB in the mid- and high-frequency ranges, respectively; also moderate attenuations up to 5 dB occurred in the aft quadrant of the sideline plane. Conversely, in the forward quadrant of the flyover plane moderate amplifications were generated, while in the forward quadrant of the sideline plane amplifications up to 8 dB occurred. These large amplifications were the result of an unusually large increase in the frequency at which the spectral peak occurred (fig. 21(b)). This same phenomenon occurred in the case of configurations 1, 3, 4, and 5.

Performance.—The acoustic effects were accompanied by average reductions in the dimensionless thrust and lift coefficients of 0.02 (5%) and 0.05 (9%), respectively. These produced an average decrease of 0.05 (8%) in the flow turning efficiency and an average decrease of 1.4° in the flow turning angle.

With one exception, these test results indicate that the directivity patterns of the noise suppressions produced by the screens in the slots and ramped screen of configuration 6 are similar to those of the plug fairings and ramped screen of configuration 3, but generally the magnitudes are smaller, particularly in the mid- through very high-frequency ranges of the sideline plane where nominally 4 dB less suppression was produced. The exception occurred in the aft quadrant of the flyover plane at an X/D of 2 where the screens in the slots and ramped screen produced an average of 4 dB less noise from about the spectral peak through the very high-frequency ranges. These acoustic differences were accompanied by an average increase of 10 percent and 7 percent in the dimensionless thrust and lift coefficients, respectively, of configuration 6. Thus, configuration 6 did not respond entirely like a version of configuration 3.

Very Low-Frequency Results

An inverse relationship exists between the magnitude of the very low-frequency broadband noise attenuations and the reduced nozzle-to-flap separation distance throughout the entire noise field at which data were obtained for all the configurations tested. However, the magnitude of the attenuations varied between the configurations. In general, significant very low-frequency noise attenuations occurred between 200 and 800 hertz, however, for some configurations, the upper

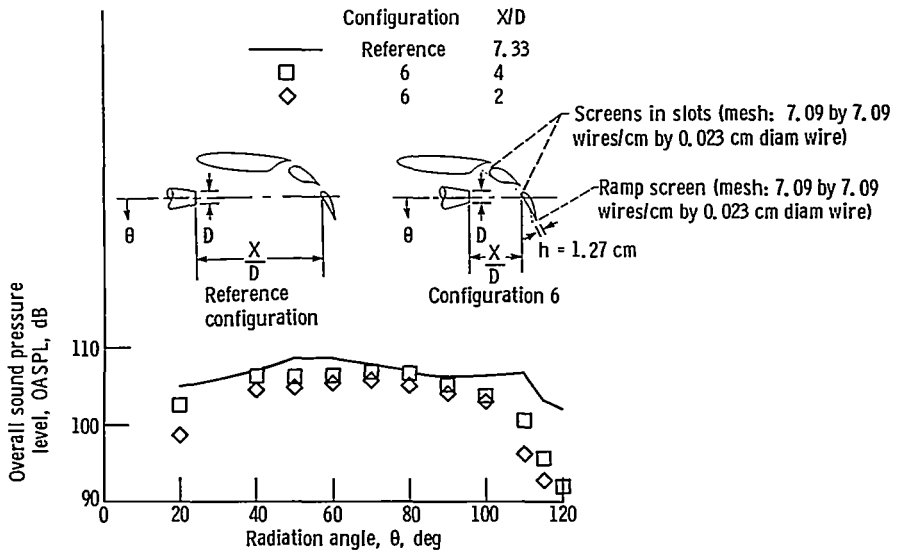

(a) Overall sound pressure level directivity.

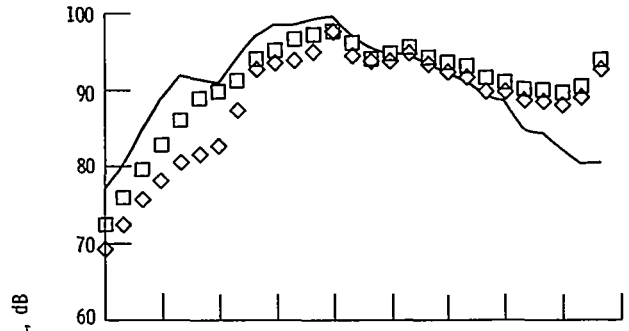

(b) Forward quadrant spectra; $\theta = 70^0$.

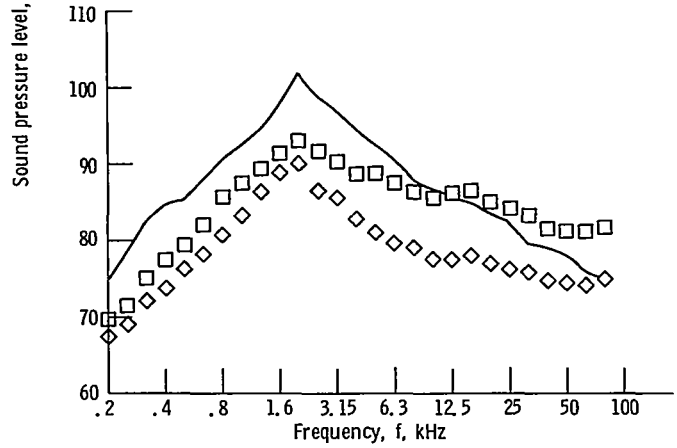

(c) Aft quadrant spectra; $\theta = 110^0$.

Figure 20. - Comparison of free-field acoustic data for reference configuration and configuration with screens over slots and ramped screen (configuration 6) in flyover plane ($\varphi = 90^0$).

limit extended to 1600 hertz. The magnitude of these attenuations varied from a low of 5 and 3.4 dB for configuration 1 at an X/D of 2 and 4, respectively, to a maximum average value of 10 dB for configuration 3 at an X/D of 2, and 6 dB for configuration 6 at an X/D of 4. These low-frequency noise suppression benefits occurred despite the lack of jet exit centerline velocity decay at the reduced nozzle to flap separation distances X/D of 2 and 4, as opposed to a 10 percent decay in the jet centerline velocity for the reference configuration, which had a separation distance X/D of 7.33. Thus, these very low-frequency noise reductions will produce

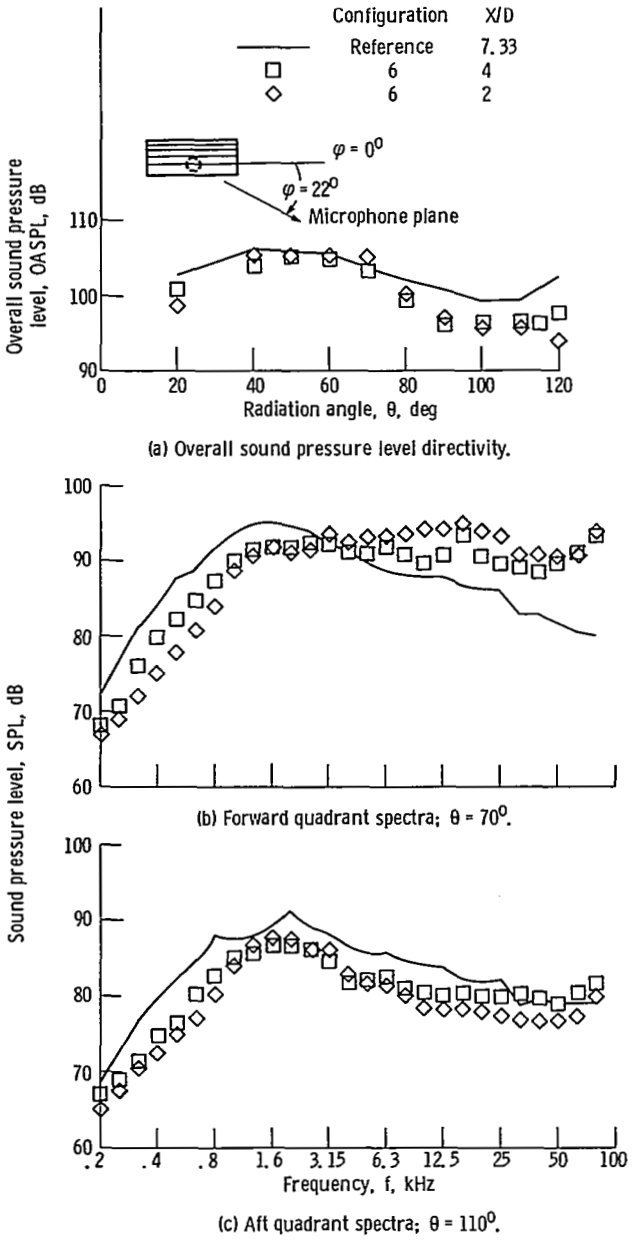

Figure 21. - Comparison of free-field acoustic data for reference configuration and configuration with screens over slots and ramped screen (configuration 6) in sideline plane ($\varphi = 22^0$).

important reductions in cabin noise and vibration in addition to reductions in structural vibration, hence metal fatigue, which will result in improved passenger comfort and safety.

Acoustic and Aerodynamic Performance at an X/D of 7.33

Additional acoustic and aerodynamic performance data were obtained with configurations 2 and 3 at an X/D of 7.33, the same separation distance as the reference configuration. This was done to determine the acoustic and aerodynamic advantages, if any, of positioning these configurations at an X/D of 7.33 instead of at the reduced separation distances. The suppression data obtained from configurations 2 and 3 located at an X/D of 7.33 were compared with that obtained at an X/D of 2 using tables I and III. A separation distance of 2 nozzle diameters was selected for the comparison because, in general, the largest noise reductions below the reference configuration occurred at this separation distance.

The results of the comparisons indicate that the principal advantage of locating configurations 2 and/or 3 at an X/D of 7.33 instead of 2 is that up to nominally 3 dB less noise was produced in the mid- and in some instances the very high-frequency ranges in the noise field, excluding the aft quadrant of the sideline plane. These attenuations were due, in part, to the decay of the jet centerline velocity at the location of the flaps, and, in part, to an observable downward shift in frequency of the spectra. Conversely, up to 5 dB more very low-frequency noise was produced throughout the entire noise field and, in some instances, in the low-frequency range of the noise field. In addition, up to 7 dB more high- and very high-frequency noise was produced in the aft quadrant of the sideline plane, where jet engine noise peaks. Finally, no significant differences in the aerodynamic performance characteristics were noted for either configuration 2 or 3 located at an X/D of 2 or 7.33.

Qualitative Effects of Suppression Devices

Based on the limited amount of parametric data presented in the preceding sections, a qualitative measure of the noise suppression and aerodynamic performance characteristics of the suppression devices alone and in combination will be discussed in this section. The noise suppression characteristics of the devices were determined by subtracting the spectral attenuations produced by each of configurations 2 through 6 from those of the reference configuration at a separation distance X/D of 7.33 and configuration 1 at an X/D of 4 and 2 using table III. The change in aerodynamic performance of the suppression devices, using table I, represents the percentage change in the turning efficiencies of configuration 2 to 6 compared to the reference configuration at an X/D of 7.33 and configuration 1 at an X/D of 4 and 2.

Effect of plugs (configuration 2).—In the flyover plane the noise reductions produced by the plug fairings of configuration 2 varied directly with some function of the separation distance throughout the spectrum. That is, the largest reductions, up to 5 dB, occurred at an X/D of 7.33 decreasing slightly at an X/D of 2. In the sideline plane no distinct trend with separation distance was found. However, the largest reductions occurred at a

separation distance of 2 nozzle diameters in the forward quadrant, while in the aft quadrant they occurred at 4 nozzle diameters. In the very low-frequency range small changes occurred except in the aft quadrant of the flyover plane where reductions of up to 5 dB occurred. Thus the noise sources throughout the entire noise field were reduced by the plugs, the reductions in the sideline plane being larger at smaller separation distances.

The changes in the aerodynamic performance characteristics of the plug fairings show that no simple relationship exists with change in separation distance. Rather, the largest reduction in turning efficiency occurred at a separation distance of 4 nozzle diameters with the lift coefficient component showing a nominal 12 percent reduction in comparison to only a small reduction in the thrust coefficient.

Combined effects of plugs and ramped screen (configuration 3).—Large very low- through high-frequency attenuations were produced by the combination of the plug fairings and ramped screen of configuration 3. In the aft quadrant of the flyover plane and throughout the sideline plane no specific trend with separation distance exists. With the exception of the aft quadrant of the sideline plane the largest noise attenuations occurred at an X/D of 2, with those at an X/D of 7.33 next. In the aft quadrant of the sideline plane comparable attenuations occurred at an X/D of 2 and 4 with smaller attenuations at an X/D of 7.33. In the flyover plane, these attenuations varied up to 10 and 4 dB in the mid- and high-frequency ranges, respectively. In the sideline plane, the attenuations varied up to 5 dB. In contrast to these attenuations, very high-frequency noise amplifications of up to nominally 2.5 dB were produced in the flyover plane and in the forward quadrant of the sideline plane. In the aft quadrant of the sideline plane, however, very high-frequency attenuations of up to 5.5 dB were produced at an X/D of 4.

The changes in aerodynamic performance characteristics of the combination of the plug fairings and ramped screen show that a weak inverse relationship exists between a reduction in the turning efficiency and the separation distance. The change is nominally equally divided between a 19 percent reduction in the lift coefficient and a 22 percent reduction in the thrust coefficient.

Effect of screen over slots (configuration 4).—At an X/D of 2 the screens of configuration 4 produced noise reductions of up to 3.5 and 2.8 dB in the forward quadrants of the flyover and sideline planes, respectively. These occurred in the low- to mid-frequency range. In the very low- and high-frequency ranges only small attenuations occurred throughout the noise field. In contrast, moderate amplifications varying up to 3.8 dB occurred in the very high-frequency range. These test results indicate that the directivity patterns of noise suppression for the screens of configuration 4 are similar to those of the nonporous plugs of configuration 2, but the magnitudes are smaller.

The aerodynamic performance characteristics of the screens over the slots showed that they produced reductions in turning efficiency that varied inversely with separation distance. The changes are a stronger function of the thrust coefficient than the lift coefficient where the lift coefficient showed an average reduction of 5 percent.

Effect of ramped screen (configuration 5).—A qualitative estimate of the noise suppression characteristics of the ramped screen of configuration 5 shows that the ramped screen produced large attenuations only in the aft quadrant of the flyover plane. At a separation distance of 2 nozzle diameters attenuations of from 5 to 10 dB occurred in the low- through the very high-frequency range, while at an X/D of 4 attenuations of from 3 to 5 dB occurred in the low- and mid-frequency ranges. Throughout the remainder of the sound field only small changes occurred in the very low- through the high-frequency range while in the very high-frequency range amplifications varied up to 4 dB, the largest occurring at an X/D of 2 in the forward quadrants of the flyover and sideline planes.

These results indicate that the ramped screen produced significant broadband suppression of a noise source that dominates the aft quadrant of the flyover plane, the magnitude of this suppression showing an inverse relationship with the nozzle to flap separation distance. In addition, significant amounts of additional very high-frequency noise were produced in the forward quadrant of the flyover plane and throughout the sideline plane.

The changes in the aerodynamic performance characteristics of the ramped screen show that no simple relationship exists with change in separation distance. Rather the largest reduction in turning efficiency of 12 percent occurred at a separation distance of 4 nozzle diameters with the thrust coefficient component showing a nominal 21 percent reduction and a 9 percent reduction in the lift coefficient.

Combined effects of screens in slots and ramped screen (configuration 6).—The screens in the slots and ramped screen of configuration 6 produced moderate to large low- through high-frequency attenuations at an X/D of 2 throughout the noise field. The largest of these occurred in the aft quadrant of the flyover plane where they varied from 7 to 10 dB in the low- through high-frequency range and nominally 4.5 dB in the very low- and very high-frequency ranges. At an X/D of 4 small to moderate attenuations occurred between the very low- and the mid-frequency ranges with the largest of these, up to 5.5 dB, occurring in the aft quadrant of the flyover plane. In contrast, with an exception at an X/D of 2 in the aft quadrant of the flyover plane, amplifications varying up to 4 dB occurred in the very high-frequency range.

The changes in aerodynamic performance characteristics of the screens in the slots and ramped screen show that no simple relationship exists with change in separation distance. Rather the largest reductions in turning efficiency occurred at separation distances of 7.33 and 2 nozzle diameters, with the lift and thrust coefficients showing nominal reductions of 14 and 13 percent respectively.

Concluding Remarks

In comparison with the reference configuration, an unusual and as yet unexplained, spectral shape appeared in the data of configurations 1, 3, 4, 5, and 6 (but not configuration 2) in the forward quadrant of the sideline plane at one or both of the reduced nozzle-to-flap separation distances. These spectra had additional mid- to very high-frequency noise that either increased the frequency at which the spectral peak occurred or produced a significant flattening or broadening of the spectral peak to higher frequencies. This effect occurred for configurations 1, 4, 5 and 6 at an X/D of 2, while it occurred for configurations 3, 5, and 6 at an X/D of 4. Thus, configurations 5 and 6 displayed the unusual spectra at both of the reduced separation distances. In the case of configurations 1, 4, 5, and 6 the spectra had a rounded shape, peaking in intensity at a significantly higher frequency than the reference configuration, while in the case of configuration 3, the spectra had one or two distinct higher frequency peaks. The phenomenon causing the rounded shaped spectra appears to occur with full or partial flow through the slots. It is also possible that it was caused by a partial separation of the flow field from one of the flaps of the EBF. If the source of this noise was removed, the noise produced by configurations 1, 4, 5, and 6 at the reduced separation distances in the forward quadrant of the sideline plane would be significantly reduced. It is considered possible that this particular source of noise may be more effectively controlled by relocating and/or changing the mesh size of the screens used in the slots between the wing and flaps.

The following general observations may be made from a comparison of the reference configuration and several of the configurations listed in tables II and III. Configuration 2 with the plug fairings positioned in the slots between the wing and flaps produced larger broadband attenuations throughout the sideline plane on the average than any of the other configurations tested, while producing a 5 percent reduction in aerodynamic turning efficiency. Configuration 3 with the plugs located in the slots between the wing and flaps and ramped screen positioned on the trailing edge of the most downstream flap produced larger broadband attenuations on the average throughout the entire noise field than any of the other configurations tested. This configuration, however, produced the poorest aerodynamic performance of the configurations tested (17 percent reduction in turning efficiency). Configuration 6 with the screens located over the slots between the wing and flaps and a ramped screen located on the trailing edge of the most downstream flap, and configuration 5 having a ramped screen located on the trailing edge of the most downstream flap produced larger broadband attenuations in the aft quadrant of the flyover plane than any of the other configurations. Finally, two possible disadvantages of reducing the separation distance between an engine nozzle exhaust plane and the flaps of a full scale UTW EBF aircraft are high surface temperatures resulting from a higher temperature (less diffused) jet impinging on the flaps' surfaces, and engine back pressure effects producing variations in mass flow rate.

Summary of Results

Small scale model acoustic tests of an engine under-the-wing externally blown flap configuration were conducted in the approach attitude with and without several passive types of noise suppression devices. The objective was to demonstrate the noise suppression effectiveness produced with and without these devices at several nozzle to flap separation distances. In addition, a qualitative estimate of the noise suppression characteristics of the individual noise suppression devices used in these tests was made. Finally static aerodynamic performance data were presented for the configurations considered. The major results of this study are as follows:

1. Broadband very low-frequency noise reductions up to 8 dB were produced throughout the entire noise field by reducing the separation distance between the nozzle and flaps of a representative under the wing externally blown flap configuration in its approach attitude. These results are consistent with the ideas expressed in references 8 and 9, which proposed that by positioning the flaps closer to the nozzle exit plane attenuation of the broadband low-frequency noise should occur. An inverse relationship exists between the magnitude of these broadband noise reductions and the nozzle-to-flap separation distance for all the configurations tested. In general, these noise reductions were augmented by the suppression devices used in this study.

2. Moderate mid- through very high-frequency noise attenuations occurred in the aft quadrant of the sideline plane for the unsuppressed configuration at reduced separation distance. Conversely, large mid-frequency amplifications were generated only in the forward quadrant of the sideline plane at a separation distance of 2 nozzle diameters. In addition, average increases of 6 percent in the flow turning efficiency over those of the reference configuration were produced.

3. Application of the three passive types of suppression devices singularly or in combination produced a complex set of results, the most important of which are summarized as follows:

(a) The configuration with the plugs in the slots between the wing and flaps produced moderate mid-frequency attenuations in the forward quadrant of the flyover plane, and large mid- through very high-frequency attenuations in the aft quadrant of the sideline plane. Moderate amplifications occurred in the mid- through very high-frequency range in the forward quadrant of the the sideline plane. A 5 percent reduction was produced in the aerodynamic performance flow turning efficiency.

(b) The configuration having the plugs in the slots and a ramped screen on the trailing edge of the most downstream flap produced large attenuations in the mid-frequency range throughout the flyover plane, and in the mid- through very high-frequency range in the aft quadrant of the sideline plane. Moderate high- and very high-frequency amplifications were produced in the forward quadrant of the sideline plane. A 17 percent reduction was produced in the aerodynamic performance flow turning efficiency.

(c) The configuration having the screens over the slots produced moderate attenuations in the mid- through very high-frequency range only in the aft quadrant of the sideline plane. Large very high-frequency amplifications occurred in the forward quadrant of the flyover plane, and large mid- through very high-frequency amplifications were produced in the forward quadrant of the sideline plane. No change occurred in the aerodynamic performance flow turning efficiency.

(d) The configuration having a ramped screen on the trailing edge of the most downstream flap produced large mid- through high-frequency attenuations in the aft quadrant of the flyover plane with small attenuations in the aft quadrant of the sideline plane. Moderate to large mid- through very high-frequency amplifications were generated in the forward quadrants of the flyover and sideline planes. A 5 percent reduction was produced in the aerodynamic performance flow turning efficiency.

(e) The configuration having screens over the slots between the wing and flaps and a ramped screen on the trailing edge of the most downstream flap produced large mid- through very high-frequency attenuations in the aft quadrant of the flyover plane, while also producing moderate, mid- through very high-frequency attenuations in the aft quadrant of the sideline plane. Moderate high- and very high-frequency amplifications occurred in the forward quadrant of the flyover plane, and large mid- through high-frequency amplifications were produced in the forward quadrant of the sideline plane. An 8 percent decrease was produced in the aerodynamic performance flow turning efficiency.

Lewis Research Center
National Aeronautics and Space Administration
Cleveland, Ohio, January 20, 1981

Appendix—Symbols

D	diameter, m
f	frequency, Hz
F_a	thrust, N
F_N	lift, N
h	ramp screen height (see figs. 5 and 7), cm
OASPL	overall sound pressure level, dB
PNL	perceived noise level, PNdB
SPL	sound pressure level, dB
T	ideal nozzle thrust, N
X	separation distance between nozzle exit plane and intersection of the nozzle axis with the most downstream flap, m
η	turning efficiency represents the square root of the sum of the squares of the dimensionless lift F_N/T, and dimensionless thrust F_a/T
θ	radiation angle measured from nozzle inlet, deg
φ	azimuthal angle; angle measured between a plane passing through the span of the wing parallel to the axis of the nozzle and the microphone plane (see fig. 3), deg

References

1. Ciepluch, Carl: QCSEE Program Background. Quiet Power-Lift Propulsion. NASA CP-2077, 1978, pp. 1-16.
2. Maglieri, Domenic J.; and Hubbard, Harvey H.: Preliminary Measurements of the Noise Characteristerics of Some Jet-Augmented-Flap Configurations. NASA Memo 12-4-58L, 1959.
3. Dorsch, R.G.; Krejsa, E.A.; and Olsen, W.A.: Blown Flap Noise Research. AIAA Paper 71-745, June 1971.
4. Dorsch, R.G.: Externally Blown Flap Noise Research. SAE Paper 740468, Apr.-May 1974.
5. Loeffler, Irvin J.; Smith, Edward B.; and Sowers, Harry D.: Acoustic Design of the QCSEE Propulsion Systems. Powered-Lift Aerodynamics and Acoustics. NASA SP-406, 1976, pp. 335-356.
6. Pennock, A.P.; Swift, G.; and Marbert, J.A.: Static and Wind Tunnel Model Tests for the Development of Externally Blown Flap Noise Reduction Techniques. (LG74ER0170, Lockheed-Georgia Co., Marietta; NASA Contract NAS3-16831.) NASA CR-134675, 1975.
7. Burns, Robert J.; McKinzie, Daniel J., Jr.; and Wagner, Jack M.: Effects of Perforated Flap Surfaces and Screens on Acoustics of a Large Externally Blown Flap Model. NASA TM X-3335, 1976.
8. McKinzie, Daniel J., Jr.; Burns, Robert J.; and Wagner, Jack M.: Noise Reduction Tests of Large-Scale-Model Externally Blown Flap Using Trailing-Edge Blowing and Partial Flap Slot Covering. NASA TM X-3379, 1976.
9. McKinzie, Daniel J., Jr.; and Burns, Robert J.: Analysis of Noise Produced by Jet Impingement Near the Trailing Edge of a Flat and a Curved Plate. NASA TM X-3171, 1975.
10. Neuwerth, G.: Acoustic Feedback Phenomena of the Subsonic and Hypersonic Free Jet Impinging on a Foreign Body. NASA TT F-15719, 1974.
11. Kadman, Y.; and Chandiramani, K.L.: EBF Noise Reduction Through Nozzle/Flap Positioning. Powered-Lift Aerodynamics and Acoustics. NASA SP-406, 1976, pp. 307-324.
12. Olsen, W.; Burns, R.; and Groesbeck, D.: Flap Noise and Aerodynamic Results for Model QCSEE Over-the-Wing Configurations. NASA TM-73588, 1977.
13. von Glahn, U.; and Groesbeck, D.: Effect of External Jet-Flow Deflector Geometry on OTW Aero-Acoustic Characteristics. AIAA Paper 76-499, July 1976.
14. Dorsch, Robert G.; Kreim, Walter J.; and Olsen, William A.: Externally-Blown-Flap Noise. AIAA Paper 72-129, Jan. 1972.
15. Shields, F. Douglas; and Bass, H.E.: Atmospheric Absorption of High Frequency Noise and Application to Fractional-Octave Bands. NASA CR-2760, 1977.
16. Wazyniak, Joseph A.; Shaw, Loretta M.; and Essary, Jefferson D.: Characteristics of an Anechoic Chamber for Fan Noise Testing. NASA TM X-73555, 1977.
17. McKinzie, D.J., Jr.: EBF Noise Suppression and Aerodynamic Penalties. AIAA Paper No. 78-240, Jan. 1978.
18. McKinzie, D.J., Jr.: Measured and Predicted Impingement Noise for a Model Scale Under-the-Wing Externally Blown Flap Configuration with a QCSEE-Type Nozzle. NASA TM-81494, 1980.
19. von Glahn, U.H.; Groesbeck, D.E.; and Huff, R.G.: Peak Axial-Velocity Delay with Single- and Multiple-Element Nozzles. AIAA Paper 72-48, Jan. 1972.

1. Report No.	2. Government Accession No.	3. Recipient's Catalog No.
NASA TP-1995		

4. Title and Subtitle	5. Report Date
AEROACOUSTIC PERFORMANCE OF AN EXTERNALLY BLOWN FLAP CONFIGURATION WITH SEVERAL FLAP NOISE SUPPRESSION DEVICES	May 1982
	6. Performing Organization Code 505-32-02
7. Author(s) Daniel J. McKinzie, Jr.	8. Performing Organization Report No. E-573
9. Performing Organization Name and Address National Aeronautics and Space Administration Lewis Research Center Cleveland, Ohio 44135	10. Work Unit No.
	11. Contract or Grant No.
12. Sponsoring Agency Name and Address National Aeronautics and Space Administration Washington, D.C. 20546	13. Type of Report and Period Covered Technical Paper
	14. Sponsoring Agency Code

15. Supplementary Notes

16. Abstract

Small-scale model acoustic experiments were conducted to measure the noise produced in the flyover and sideline planes by an engine under-the-wing externally blown flap configuration in its approach attitude. Broadband low frequency noise reductions as large a 9 dB were produced by reducing the separation distance between the nozzle exhaust plane and the flaps. Experiments were also conducted to determine the noise suppression effectiveness in comparison with a reference configuration of three passive types of devices that were located on the jet impingement surfaces of the reference configuration. These devices produced noise reductions that varied up to 10 dB at reduced separation distances. In addition, a qualitative estimate of the noise suppression characteristics of the separate devices was made. Finally static aerodynamic performance data were obtained to evaluate the penalties incurred by these suppression devices. The test results suggest that further parametric studies are required in order to understand more fully the noise mechanisms that are affected by the suppression devices used in this study.

17. Key Words (Suggested by Author(s))	18. Distribution Statement
Acoustics V/STOL Propulsion Noise	Unclassified - unlimited STAR Category 71

19. Security Classif. (of this report)	20. Security Classif. (of this page)	21. No. of Pages	22. Price*
Unclassified	Unclassified	29	A04

* For sale by the National Technical Information Service, Springfield, Virginia 22161

NASA-Langley, 1982

National Aeronautics and
Space Administration

Washington, D.C.
20546

Official Business
Penalty for Private Use, $300

THIRD-CLASS BULK RATE

Postage and Fees Paid
National Aeronautics and
Space Administration
NASA-451

U.S.MAIL

1 1 1U,H, 043082 S00903DS
DEPT OF THE AIR FORCE
AF WEAPONS LABORATORY
ATTN: TECHNICAL LIBRARY (SUL)
KIRTLAND AFB NM 87117

NASA

POSTMASTER: If Undeliverable (Section 158 Postal Manual) Do Not Return